GraphMaster: Automated Graph Synthesis via LLM Agents in Data-Limited Environments

Enjun Du¹, Xunkai Li¹, Tian Jin², Zhihan Zhang¹, Rong-Hua Li¹, Guoren Wang¹

Beijing Institute of Technology

The Hong Kong University of Science and Technology (Guangzhou)

Abstract

The era of foundation models has revolutionized AI research, yet Graph Foundation Models (GFMs) remain constrained by the scarcity of large-scale graph corpora. Traditional graph data synthesis techniques primarily focus on simplistic structural operations, lacking the capacity to generate semantically rich nodes with meaningful textual attributes—a critical limitation for real-world applications. While large language models (LLMs) demonstrate exceptional text generation capabilities, their direct application to graph synthesis is impeded by context window limitations, hallucination phenomena, and structural consistency challenges. To address these issues, we introduce **GraphMaster**—the first multi-agent framework specifically designed for graph data synthesis in data-limited environments. GraphMaster orchestrates four specialized LLM agents (Manager, Perception, Enhancement, and Evaluation) that collaboratively optimize the synthesis process through iterative refinement, ensuring both semantic coherence and structural integrity. To rigorously evaluate our approach, we create new data-limited "Sub" variants of six standard graph benchmarks, specifically designed to test synthesis capabilities under realistic constraints. Additionally, we develop a novel interpretability assessment framework that combines human evaluation with a principled Grassmannian manifold-based analysis, providing both qualitative and quantitative measures of semantic coherence. Experimental results demonstrate that GraphMaster significantly outperforms traditional synthesis methods across multiple datasets, establishing a strong foundation for advancing GFMs in data-scarce environments.²

1 Introduction

In the era of foundation models, unprecedented advances in natural language processing and computer vision have been enabled by massive training corpora [51, 49, 52, 50, 38, 53, 60, 46]. Graph Foundation Models (GFMs) [26, 23, 38, 53] represent a promising frontier for AI in graph-structured data, yet their development faces a critical bottleneck: the scarcity of large-scale, diverse graph datasets. Unlike text and image domains where data collection is relatively straightforward, gathering and annotating graph data often requires specialized expertise and significant resources. This data quantity constraint has become the primary challenge for training robust GFMs, particularly as model size increases and demands exponentially more training examples for optimal performance.

Graph data synthesis offers a strategic solution to this fundamental constraint by automatically generating new graph samples that maintain both semantic richness and structural validity. Existing synthesis approaches, however, face substantial limitations. Edge-level operations [57, 59] manipulate existing connections but cannot create novel nodes or patterns. Node-level mixing techniques like

^{*} Corresponding author

²Code is available on https://github.com/EnjunDu/GraphMaster.

GraphMixup [47] generate synthetic nodes by interpolating features but often produce semantically inconsistent attributes, particularly with textual features. Graph-level synthesis methods such as G-Mixup [14] create entirely new graphs but struggle to balance global structure with local semantic coherence. The core limitation across these traditional methods is their inability to simultaneously preserve meaningful semantics while generating structurally valid expansions—a deficiency particularly pronounced when handling text-attributed graphs (TAGs) where both connectivity patterns and textual node features must remain coherent.

Large language models have demonstrated remarkable capabilities in understanding and generating text [15, 9, 55, 20, 2, 40], suggesting potential for synthesizing text-attributed graphs. However, directly applying LLMs encounters several critical challenges: standard context windows cannot process entire graphs with numerous textual nodes [3]; LLMs excel at semantic understanding but struggle to maintain structural consistency [10]; and without proper coordination, they tend to produce inconsistent or hallucinated content that fails to capture the intricate balance between topology and semantics [28]. Furthermore, in realistic scenarios with limited available data, LLMs have insufficient examples to learn complex graph patterns [22, 39, 21].

To address these challenges, we propose **GraphMaster**, a novel multi-agent framework specifically designed for graph synthesis in data-limited environments. GraphMaster decomposes the complex synthesis task into specialized sub-tasks handled by four collaborative LLM-powered agents, each targeting specific challenges: (1) The Manager Agent coordinates the overall process and determines optimal synthesis strategies based on current graph characteristics, orchestrating the complex synthesis workflow; (2) The Perception Agent analyzes graph structure and employs advanced sampling to identify representative subgraphs processable within LLM context constraints, directly addressing the context window limitations; (3) The Enhancement Agent generates new nodes and edges with consistent semantics and structure, mitigating hallucination by maintaining coherence with existing graph elements; and (4) The Evaluation Agent assesses quality based on both semantic coherence and structural integrity, providing feedback for iterative improvement to ensure structural and semantic consistency. This decomposition enables targeted solutions for each challenge that a single-pass LLM approach cannot address.

Through this collaborative, iterative process, these specialized agents overcome the limitations of both traditional methods and direct LLM applications. The multi-agent architecture enables GraphMaster to effectively balance semantic richness with structural validity—producing high-quality synthetic graph data even with limited training examples. By introducing modular reasoning (through task decomposition), semantic control (via specialized agent expertise), and iterative optimization (through feedback cycles), GraphMaster achieves synthesis capabilities beyond what single-pass approaches can deliver.

Our contributions can be summerized as follows:

- New perspective for LLM-based TAG Synthesis: we first propose a novel multi-agent framework from the RAG perspective to synthesize TAG under data-limited environment. By integrating context retrieval with iterative feedback, this new perspective enables both semantic richness and structural fidelity.
- **Groundbreaking Benchmark**: We introduce a standardized "Data-limited" variant testbed for text-attributed graph synthesis and develop a dual-perspective interpretability assessment—combining expert human evaluation with Grassmann manifold-based analysis—to provide reproducible comparisons and deep semantic-structural insights.
- **State-of-the-Art Performance**: Extensive experiments on multiple datasets and GNN architectures demonstrate that our method consistently outperforms existing baselines, setting a new benchmark for data-limited TAG synthesis.

2 Background Methods

2.1 Classic Graph Data Synthesis Methods

Traditional graph data synthesis methods [7] address data scarcity through various approaches. Edgelevel operations [57] modify topology by adding or deleting connections. Node-level techniques like GraphSMOTE [56] generate new nodes through minority class interpolation. Graph-level methods

such as G-Mixup [14] create entirely new graph instances via graphon interpolation. Interpolation-based approaches [35, 34] combine hidden representations to enhance model robustness. Despite their diversity, these methods primarily focus on structural manipulations without generating semantically meaningful textual attributes.

2.2 LLM-based Multi-Agent Systems for Data Generation

Recent LLM-powered multi-agent frameworks demonstrate capabilities for complex data generation tasks. General collaboration systems like Self-Instruct [36] and distributed simulation platforms [29] establish architectures for coordinated AI systems. In graph contexts, approaches like GoG [42] and LLM-based social simulations [16] leverage semantic understanding for graph-related tasks. However, specific applications for text-attributed graph synthesis in data-limited environments remain largely unexplored.

2.3 Problem Formulation: Graph Data Synthesis

Text-Attributed Graphs. We formally define a text-attributed graph (TAG) as $\mathcal{G} = (\mathcal{V}, \mathcal{E}, \mathcal{X}, \mathcal{Y})$, where $\mathcal{V} = \{v_1, v_2, \dots, v_N\}$ is a set of N nodes, $\mathcal{E} \subseteq \mathcal{V} \times \mathcal{V}$ is the set of edges with corresponding adjacency matrix $\mathcal{A} \in \{0, 1\}^{N \times N}$, $\mathcal{X} = \{x_1, x_2, \dots, x_N\}$ is the set of textual features with each x_i corresponding to node $v_i \in \mathcal{V}$, and $\mathcal{Y} = \{y_1, y_2, \dots, y_N\}$ represents the set of node labels where $y_i \in \{1, 2, \dots, C\}$ for C distinct classes.

Knowledge Extraction. Given the context length constraints of LLMs, we define a knowledge extraction function $\Phi: \mathcal{G} \to \mathcal{K}$ that samples a representative subgraph as:

$$\mathcal{K} = \Phi(\mathcal{G}) = (\mathcal{V}_k, \mathcal{E}_k, \mathcal{X}_k, \mathcal{Y}_k), \tag{1}$$

where $V_k \subset V$, $\mathcal{E}_k = \{(v_i, v_j) \in \mathcal{E} \mid v_i, v_j \in \mathcal{V}_k\}$, and $\mathcal{X}_k, \mathcal{Y}_k$ are the corresponding text attributes and labels. The extraction function Φ employs specialized sampling strategies to ensure \mathcal{K} captures both structural and semantic characteristics of \mathcal{G} while remaining within LLM context limits.

Graph Synthesis Process. The graph synthesis process is formalized as a function $\Psi : \mathcal{K} \to \mathcal{G}_s$ that generates new graph elements based on the extracted knowledge:

$$\mathcal{G}_s = \Psi(\mathcal{K}) = (\mathcal{V}_s, \mathcal{E}_s, \mathcal{X}_s, \mathcal{Y}_s), \tag{2}$$

where G_s represents the synthesized graph components. Function Ψ is implemented through our framework that encompasses both semantic understanding and structural pattern recognition.

Graph Synthesis. The final enhanced graph merges the original and synthesized components:

$$\mathcal{G}_{\text{new}} = \mathcal{G} \oplus \mathcal{G}_s = (\mathcal{V} \cup \mathcal{V}_s, \mathcal{E} \cup \mathcal{E}_s \cup \mathcal{E}_c, \mathcal{X} \cup \mathcal{X}_s, \mathcal{Y} \cup \mathcal{Y}_s), \tag{3}$$

where $\mathcal{E}_c = \{(v_i, v_j) \mid v_i \in \mathcal{V}, v_j \in \mathcal{V}_s\}$ represents newly created edges connecting original and synthetic nodes. The quality of \mathcal{G}_{new} is evaluated based on both semantic coherence (how well \mathcal{X}_s aligns with original textual patterns) and structural fidelity (how well \mathcal{E}_s and \mathcal{E}_c preserve the topological characteristics of \mathcal{G}).

3 The Proposed Method

We present GraphMaster, a multi-agent framework conceptualized through the lens of Retrieval-Augmented Generation (RAG) [44, 48] to address the challenges of graph synthesis in data-constrained environments. As illustrated in Figure 1, GraphMaster implements a hierarchical RAG paradigm wherein four specialized LLM-powered agents operate collaboratively in a recursive optimization loop to generate semantically rich and structurally coherent graph extensions.

3.1 Framework Overview: RAG-Based Multi-Agent Architecture

GraphMaster formalizes graph synthesis as an iterative RAG process, operating through specialized agents in a closed-loop optimization system. While a single LLM might possess the theoretical capability to understand graph structures, the inherent complexity of generating coherent graph data

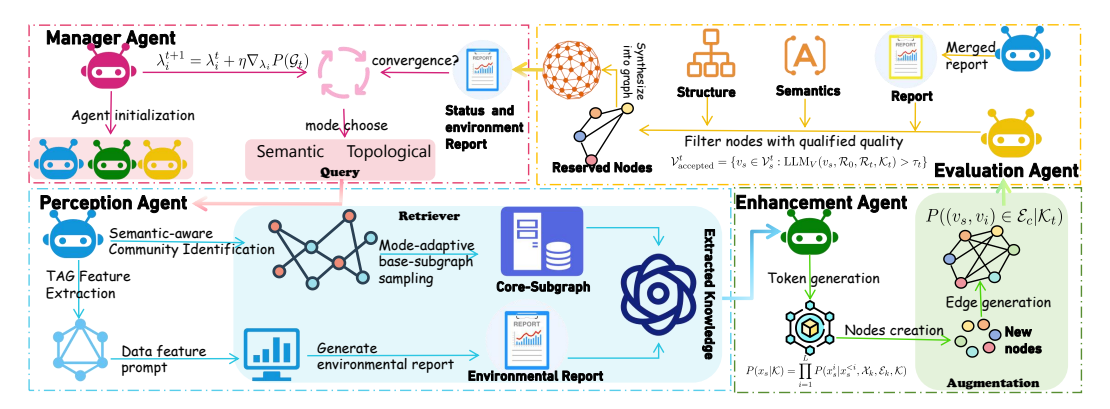


Figure 1: GraphMaster: A hierarchical multi-agent framework for text-attributed graph synthesis.

necessitates a specialized multi-agent approach for three critical reasons. First, real-world graphs substantially exceed typical LLM context windows, requiring strategic sampling and knowledge extraction. Second, maintaining structural consistency across generated elements demands focused attention on connectivity patterns that single-pass generation cannot guarantee. Third, controlling hallucination requires continuous evaluation and refinement through iterative feedback. A collaborative multi-agent architecture effectively addresses these challenges through specialization and integration:

$$\mathcal{G}_{\text{new}} = \Psi_{\text{RAG}}(\mathcal{G}, \mathcal{Q}, \mathcal{R}, \mathcal{A}_{\text{retrieve}}, \mathcal{A}_{\text{generate}}, \mathcal{A}_{\text{evaluate}})$$
(4)

where \mathcal{G} is the original graph, \mathcal{Q} represents the query formulation (enhancement mode), \mathcal{R} denotes the retrieval strategy, and $\mathcal{A}_{retrieve}$, $\mathcal{A}_{generate}$, and $\mathcal{A}_{evaluate}$ correspond to the agent-specific functions for retrieval, generation, and evaluation, respectively. In each iteration, the Manager Agent formulates the query to guide the synthesis process, the Perception Agent retrieves relevant context to overcome context window limitations, the Enhancement Agent generates new content while maintaining structural consistency, and the Evaluation Agent assesses quality and addresses potential hallucinations—with this cycle continuing until convergence. This collaborative framework enables each agent to focus on a specific challenge while collectively producing coherent graph extensions that a single-pass approach cannot achieve.

3.2 Manager Agent: Query Optimization and Control Mechanism

The Manager Agent serves as the meta-cognitive controller that formulates the synthesis query \mathcal{Q}_t at iteration t based on a comprehensive environmental status report $\mathcal{R}_t = \mathrm{LLM}_P(\mathcal{G}_t)$ generated by the Perception Agent. The mode selection function is formalized as: $M_t = \mathrm{LLM}_M(\mathcal{R}_t) \in \{\text{semantic}, \text{topological}\}$ where LLM_M represents the Manager Agent's reasoning process that analyzes community structures and label distributions captured in \mathcal{R}_t . This query formulation implements an adaptive mechanism where the Manager optimizes a multi-objective utility function:

$$\omega_t^* = \underset{\omega \in \Omega}{\arg \max} \left[\lambda_1 U_{\text{sem}}(\omega, \mathcal{G}_t) + \lambda_2 U_{\text{struct}}(\omega, \mathcal{G}_t) + \lambda_3 U_{\text{bal}}(\omega, \mathcal{G}_t) \right]$$
 (5)

where Ω is the strategy space, U_{sem} , U_{struct} , and U_{bal} represent semantic coherence, structural integrity, and class balance utilities respectively, with adaptive weights λ_i that evolve according to: $\lambda_i^{t+1} = \lambda_i^t + \eta \nabla_{\lambda_i} P(\mathcal{G}_t)$ where $P(\mathcal{G}_t)$ measures synthesis progress and η is a learning rate. The Manager orchestrates state transitions, modeled as $s_{t+1} = T(s_t, a_t, M_t)$, where states s_t reflect graph composition and actions $a_t \in \{a_P, a_E, a_V\}$ correspond to agent invocations for Perception, Enhancement, and Evaluation respectively.

3.3 Perception Agent: Context-Aware Corpus Retrieval

The Perception Agent implements the retrieval component of the RAG paradigm, extracting a relevant subgraph from the input graph \mathcal{G}_t based on the query $\mathcal{Q}_t = M_t$. This retrieval process is formalized

as: $\mathcal{K}_t = \mathscr{R}(\mathcal{G}_t, \mathcal{Q}_t) = (\mathcal{V}_k, \mathcal{E}_k, \mathcal{X}_k, \mathcal{Y}_k)$ where \mathcal{K}_t represents the retrieved knowledge capsule. The retrieval function \mathscr{R} operates through three sequential stages:

Semantic-aware Community Identification: The agent employs a semantic-enriched modularity maximization algorithm to calculate the community distribution of semantic associations for TAG:

$$Q_{\text{sem}} = \frac{1}{2m} \sum_{i,j} \left[\mathcal{A}_{ij} - \gamma \frac{k_i k_j}{2m} - (1 - \gamma) \frac{d_{\text{sem}}(x_i, x_j)}{\sum_{l,m} d_{\text{sem}}(x_l, x_m)} \right] \delta(c_i, c_j)$$
(6)

where $d_{\text{sem}}(x_i, x_j) = \frac{\mathbf{x}_i \cdot \mathbf{x}_j}{\|\mathbf{x}_i\| \|\mathbf{x}_j\|}$ computes semantic similarity between node attributes, k_i and k_j represent the degrees of nodes i and j, and γ balances topological and semantic factors.

Mode-Adaptive Seed Selection Strategy: Based on the enhancement mode M_t , the agent selects an optimal seed community C_b :

$$C_b = \begin{cases} \underset{i}{\operatorname{arg \, min}} |C_i| \cdot (1 + \mu \cdot \operatorname{Var}(\{x_j : v_j \in C_i\})), & \text{if } M_t = \text{semantic}, \\ \{v_j \in \mathcal{V}_{\text{train}} : y_j = \underset{c}{\operatorname{arg \, max}} \phi_{\text{imbal}}(c)\}, & \text{if } M_t = \text{topological} \end{cases}$$
(7)

where $\phi_{\text{imbal}}(c) = \max_{c'} |\mathcal{V}_{c'}|/|\mathcal{V}_c|$ quantifies class imbalance, Var denotes the variance of node textual features within a community and μ weights semantic variance importance. For semantic synthesis, the smaller communities with low internal semantic variance are prefer to be selected to establish a cohesive foundation. For topological synthesis, nodes from minority classes are prioritized.

Hierarchical Stochastic Diffusion Sampling: The agent employs a mode-conditional Personalized PageRank (PPR) algorithm, defined as $\pi^{(k+1)} = \alpha v + (1-\alpha)W^T\pi^{(k)}$, where the teleportation vector v varies by enhancement mode: $v_i = \frac{1}{|\mathcal{C}_b|}$ if $v_i \in \mathcal{C}_b$ and $M_t = \text{semantic}$, or $v_i = \frac{\mathbb{I}[y_i = \hat{y}]}{\sum_j \mathbb{I}[y_j = \hat{y}]}$ if $v_i \in \mathcal{V}_{\text{train}}$ and $M_t = \text{topological}$, where $\hat{y} = \arg\min_{c} |\{v_j \in \mathcal{V}_{\text{train}} : y_j = c\}|$ identifies the label with minimal representation. Following diffusion convergence, the final knowledge subgraph is selected as:

$$\mathcal{K}_t = \{ v_i \in \mathcal{S}_{\text{top-}K\%} : r_i < \min(1, \beta \cdot \boldsymbol{\pi}_i / \max_j \boldsymbol{\pi}_j) \} \cap \mathcal{S}_{\text{diverse}}$$
 (8)

where $|\mathcal{K}_t| = N$ is constrained by the LLM context window, $\mathcal{S}_{\text{top-}K\%}$ contains the top K% nodes by PPR score, $r_i \sim \text{Uniform}(0,1)$ introduces controlled stochasticity, and $\mathcal{S}_{\text{diverse}}$ ensures community coverage. The environmental status report \mathcal{R}_t encapsulates multi-scale graph properties:

$$\mathcal{R}_t = \left(\rho_{\text{global}}, \{\rho_{\text{class}}^c\}_{c=1}^C, \{\rho_{\text{comm}}^i\}_{i=1}^{|\mathcal{C}|}, \mathcal{D}_{\text{struct}}, \mathcal{D}_{\text{sem}}\right)$$
(9)

where ρ_{global} captures global statistics, ρ_{class}^c and ρ_{comm}^i encode class-level and community-level properties, while $\mathcal{D}_{\mathrm{struct}}$ and $\mathcal{D}_{\mathrm{sem}}$ represent structural and semantic distributions.

3.4 Enhancement Agent: Context-Conditioned Generation

The Enhancement Agent implements the generation component of the RAG paradigm, synthesizing new graph elements (no more than M% of the knowledge subgraph) based on the retrieved knowledge and environmental report. The synthesis process follows Eq. (2) where $\mathcal{K} = (\mathcal{K}_t, \mathcal{R}_t, M_t)$. For semantic mode, the LLM generates node attributes using a conditional autoregressive model:

$$P(x_s|\mathcal{K}) = \prod_{i=1}^{L} P(x_s^i|x_s^{< i}, \mathcal{X}_k, \mathcal{E}_k, \mathcal{K})$$
(10)

where x_s^i is the *i*-th token of attribute x_s , and L is the sequence length. This formulation enables the LLM to generate coherent textual attributes that maintain consistency with the knowledge subgraph while introducing appropriate variations.

Crucially, regardless of the current enhancement mode, the agent always generates both node attributes and their connections. For topological mode, the LLM models edge connections between new node v_s and existing nodes by estimating the probability:

$$P((v_s, v_i) \in \mathcal{E}_c | \mathcal{K}) = \sigma \left(\theta_1 \cdot \sin(x_s, x_i) + \theta_2 \cdot \frac{|\mathcal{N}(v_i) \cap \mathcal{N}_K(v_s)|}{|\mathcal{N}_K(v_s)|} + \theta_3 \cdot \frac{k_i}{\max_j k_j} \right)$$
(11)

where $\mathcal{N}(v_i)$ is the neighborhood of v_i , $\mathcal{N}_K(v_s)$ represents neighbors of v_s in the knowledge subgraph, and σ is the sigmoid function. The coefficients $\{\theta_j\}_{j=1}^3$ are dynamically adjusted based on the query mode M_t . This dual-mode generation enables GraphMaster to adaptively emphasize either semantic coherence or structural fidelity while maintaining integrity across both dimensions.

3.5 Evaluation Agent: Multi-dimensional Quality Assessment

The Evaluation Agent implements a comprehensive verification mechanism that integrates four critical information sources:

$$Q_t = LLM_V(\mathcal{R}_0, \mathcal{R}_t, \mathcal{K}_t, \mathcal{G}_s^t)$$
(12)

where Q_t represents the quality assessment outcome, \mathcal{R}_0 is the initial environmental report serving as a baseline, \mathcal{R}_t is the current environmental report, \mathcal{K}_t is the retrieved knowledge, and \mathcal{G}_s^t is the newly synthesized data. The Evaluation Agent simultaneously assesses two key dimensions: (i) Semantic Coherence: Evaluates whether the generated textual attributes are contextually appropriate, domain-consistent, and meaningful within the graph's thematic scope. (ii) Structural Integrity: Assesses whether the new edges form logical connections that preserve the original graph's topological patterns while addressing structural gaps.

For each generated node $v_s \in \mathcal{V}_s^t$, the LLM computes a composite quality score, with the final accepted node set defined as:

$$\mathcal{V}_{\text{accepted}}^{t} = \{ v_s \in \mathcal{V}_s^{t} : \text{LLM}_V(v_s, \mathcal{R}_0, \mathcal{R}_t, \mathcal{K}_t) > \tau_t \}$$
(13)

where the threshold τ_t is adaptively updated: $\tau_t = \tau_{t-1} + \zeta(\bar{\mathcal{F}}_t(\omega_t^*) - \bar{\mathcal{F}}_{t-1}(\omega_{t-1}^*))$ with $\bar{\mathcal{F}}_t(\omega_t^*)$ representing the average quality score at iteration t. The convergence determination employs a temporal quality gradient analysis:

$$Converged_{t} = \mathbb{I}\left(\max_{j \in \{1, \dots, k\}} |\bar{\mathcal{F}}_{t}(\omega_{t}^{*}) - \bar{\mathcal{F}}_{t-j}(\omega_{t-j}^{*})| < \epsilon \wedge LLM_{goal}(\mathcal{R}_{0}, \mathcal{R}_{t}) = True\right)$$
(14)

where $\mathbb{I}(\cdot)$ is the indicator function and LLM_{goal} assesses whether synthesis objectives have been achieved. If convergence is detected, the Evaluation Agent signals task completion to the Manager Agent; otherwise, it triggers another iteration of the synthesis process³.

3.6 Time Complexity Analysis

The time complexity of GraphMaster is dominated by three operations: (1) community detection and PPR computation in the Perception Agent, which run in near-linear time $O(|V_t| + |E_t|)$ on the current graph; (2) LLM inference for node attribute generation and edge probability estimation, which scales with the size N of the retrieved subgraph rather than the full graph; and (3) quality assessment, which evaluates a fixed number of newly generated nodes against predetermined criteria. Since N is constrained by the LLM context window and typically small relative to $|V_t|$, the LLM operations remain efficient regardless of overall graph size. If the iterative process runs for T iterations before convergence (generally small due to the Evaluation Agent's stringent criteria), the overall complexity is T times the per-iteration cost. This architecture enables GraphMaster to scale effectively by leveraging LLMs for semantic generation on bounded contexts while using efficient graph algorithms for structural computations.

³We compares GraphMaster with recent remarkable graph data synthsis methods in Appendix A. Theoretical analysis of agent capabilities are given in Appendix I.

4 Experiment

To evaluate GraphMaster comprehensively, we formulate four research questions: (**RQ1**): Can GraphMaster generate high-quality text-attributed graph data in data-limited environment? (**RQ2**): Can the graph data synthesized by GraphMaster retain the original graph features well? (**RQ3**): Can GraphMaster maintain interpretability well? (**RQ4**): What is the relative contribution of each component in GraphMaster to the overall synthesis quality?

4.1 Overall Performance (RQ1)

We evaluate GraphMaster's ability to synthesize high-quality graph data by applying it to enhance the data-limited datasets we created and assessing whether the enhanced datasets improve downstream model performance. We employ standard metrics including Accuracy and F1 Score as evaluation criteria, with higher values indicating superior performance.

Baselines and Datasets. The comparative baselines are categorized into five groups: (1) original TAG training without data synthesis; (2) Classic data augmentation methods: GAugO [57]; (3) LLM-based data aigmentation methods: GraphEdit [12] and LLM4RGNN [54]; (4) Classic data synthesis methods: GraphSmote [56], G-Mixup [14], IntraMix [58], GraphAdasyn [24], FG-SMOTE [37], and AGMixup [25]; (5) LLM-based data synthesis methods: GAG [17] and LLM4NG [45], noting that there are very limited baselines for TAG synthesis using LLM, and we created these two additional baselines named Mixed-LLM and Synthesis-LLM, whose implementations can be found in the Appendix B. Our experiments utilize six widely recognized text-attributed graph datasets: Cora [27], Citeseer [11], Wikics [8], Arxiv2023 [31], and History and Children [43]. It is worth noting that in order to better simulate the data-limited environment to test the effect of data synthesis, we created 6 data-limited datasets, namely SubCora, SubCiteseer, SubWikics, SubHistory, SubArxiv2023, and SubChildren (details are given in Appendix C). In this article, unless otherwise specified, we assume that the augmentation-based method uses the original dataset, while the synthesis-based method uses the data-limited dataset we created. For downstream task evaluation, we implement four established graph neural network architectures: GCN [18], JKNET [41], GraphSage [13] and GAT [33].

Implement Details. We ran the entire experiment on eight 80G A100 GPUs, using the QwQ-32B model [32] as the base LLM and enabling it to assume different agent roles through iterative calls. For the background knowledge nodes, we set N=30, and for the newly generated nodes, we configured M%=15% (The hyperparameter selection analysis are given in Appendix E). In training the GNN model, we first initialized the text attributes with Sentence-BERT [30] to generate the initial features before proceeding with training. To ensure the robustness of our experiments, we repeated each experiment 50 times and reported the mean and standard deviation of the results.

Table 1: Comparison of GraphMaster with other TAG synthesis methods in GCN model. Best performance is indicated by the **bold** face numbers, and the <u>underline</u> means the second best. 'Acc' and 'F1' are short for Accuracy and F1 Score, respectively.

Tomo	Model	Cora		Citeseer		Wikics		History		Arxiv2023		Children	
Type		Acc	F1	Acc	F1	Acc	F1	Acc	F1	Acc	F1	Acc	F1
Original	Original Model	88.9±1.1	88.5±1.5	78.1±1.1	75.0 ± 0.3	79.7±0.8	77.8 ± 0.3	84.2±0.6	43.1±0.3	76.3±1.0	54.9±0.5	52.6±0.7	32.3±1.5
Classic-Aug	GAugO	88.9±0.8	88.0 ± 1.0	78.1±0.7	77.2 ± 0.3	79.9±0.9	77.7±0.7	84.6±1.5	44.7 ± 0.6	76.8±1.4	53.0±0.3	51.8±0.6	33.6±0.7
LLM-Aug	GraphEdit	91.0±0.9	89.7±0.6	81.9±0.9	80.8 ± 1.1	82.0±1.1	80.7 ± 1.2	87.6±0.6	45.7±1.3	78.0±0.9	57.8±0.3	54.3±0.7	35.7±1.4
LLWI-Aug	LLM4RGNN	91.2±0.6	88.8 ± 1.1	80.9±1.3	76.6 ± 1.1	83.6±1.4	81.6 ± 1.5	88.9±0.7	48.6 ± 0.4	79.3±1.1	59.1 ± 0.4	55.7±1.4	36.7 ± 0.8
	GraphSmote	88.7±1.4	87.4 ± 1.1	78.1±0.5	74.6 ± 1.4	80.7±1.5	78.6 ± 1.4	84.9±0.5	43.9 ± 0.3	76.2±0.4	55.5±0.4	53.1±0.9	33.2±0.6
	G-Mixup	87.4±1.1	87.0 ± 0.7	78.2±0.9	76.8 ± 1.1	79.7±0.4	78.0 ± 0.8	84.6±0.6	43.6 ± 0.6	76.6±0.4	56.5 ± 0.3	53.0±0.6	33.0 ± 0.3
Classic-Syn	IntraMix	80.9±0.6	82.8 ± 0.7	71.3±0.8	70.7 ± 0.5	73.7±1.0	74.5 ± 0.4	82.4±1.5	42.7 ± 0.6	72.4±1.1	53.9 ± 0.8	45.2±0.9	30.1 ± 0.7
Classic-Syli	GraphAdasyn	89.2±0.3	88.7 ± 0.5	78.9±1.0	78.4 ± 1.4	80.8±1.2	78.9 ± 0.7	84.6±1.5	46.1 ± 0.8	77.5±0.7	57.0 ± 1.1	53.6±0.5	33.0 ± 0.6
	FG-SMOTE	88.9±1.5	87.6 ± 1.0	78.7±0.8	74.7 ± 1.4	81.0±0.8	79.0 ± 1.0	85.0±1.4	44.0 ± 0.9	76.4±1.2	55.8 ± 1.4	53.1±1.5	33.3 ± 0.9
	AGMixup	84.7±0.4	86.6 ± 0.4	71.7±0.9	73.2 ± 1.1	78.8±0.9	76.6 ± 1.1	81.8±0.9	42.9 ± 0.3	76.8±1.1	53.7±0.5	53.6±1.0	32.6 ± 0.8
	GAG	91.0±1.2	89.3±0.4	82.8±0.9	80.0 ± 1.5	84.9±1.3	83.2±0.7	88.9±0.5	49.8±0.8	79.9±0.5	59.4±1.0	56.7±0.8	38.0±0.5
	LLM4NG	85.9±0.3	84.0 ± 0.2	73.9±0.2	72.0 ± 0.3	72.8±0.1	72.9 ± 0.4	82.5 ±0.5	48.4 ± 0.3	79.0 ± 0.2	61.2 ± 0.5	44.6 ± 0.2	27.2 ± 0.4
LLM-Syn	Mixed-LLM	89.9±0.5	89.3 ± 0.4	83.5±0.9	81.3 ± 0.8	84.9±0.9	83.4 ± 0.8	89.2±1.3	55.8±0.8	81.4±1.5	61.2 ± 0.9	60.0±0.7	39.6 ± 0.7
	Synthesis-LLM	89.8±1.3	89.1 ± 1.0	84.5±1.0	82.7 ± 1.1	84.8±0.4	83.2±0.5	89.4±1.3	53.4±1.3	81.0±1.2	62.3 ± 0.8	60.9±1.0	40.1 ± 0.9
	GraphMaster	93.7 ± 1.0	92.5 ± 1.0	88.3±0.9	87.7±1.1	87.9±0.8	86.8 ± 0.9	92.6±1.3	63.4±1.4	87.9±1.3	66.3±1.5	68.8±1.4	47.8±1.3

Results. As shown in Table 1 (Due to space limitation, other three models' results are given in Appendix F.), GraphMaster consistently outperforms all baselines, demonstrating the superiority of our approach. Notably, we observed that some baseline methods even yield lower performance than the original dataset. This is primarily because traditional graph synthesis techniques fail to capture the semantic nuances of sentences; consequently, when using Sentence-BERT embeddings

instead of bag-of-words representations, their effectiveness is significantly diminished. Moreover, the other LLM-based baselines we compared against mainly focus on anti-interference detection or data synthesis on other scenarios rather than TAG data synthesis, resulting in their performance being significantly lower than that of GraphMaster, which targets TAG data synthesis. Finally, the two LLM-based TAG synthesis baselines we developed show significant advantages over traditional baselines. However, since they cannot fully understand the semantics and topological structure of TAG, although they are higher than other baselines, they are still significantly lower than GraphMaster⁴.

4.2 Synthetic Graph Feature Analysis (RQ2)

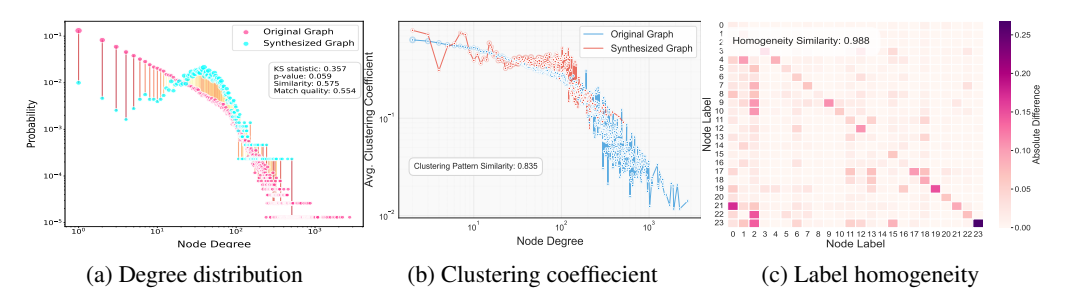


Figure 2: Graph feature analysis on Children dataset.

Our second research question examines whether the new graph data generated by GraphMaster in data-limited environments can maintain consistency with the original graph's structural features. We conducted a comprehensive analysis across three dimensions: degree distribution, clustering coefficient, and label homogeneity. As shown in Figure 2, GraphMaster demonstrates excellent performance in preserving the network's topological backbone. For example, the two-sample Kolmogorov–Smirnov test statistic between the degree distributions of the original and synthesized Children graphs is 0.357 (p=0.059), indicating no statistically significant difference. The clustering coefficient similarity score is 0.835, which represents a substantial improvement over the original data-limited Children graph (0.785). Concurrently, the label homogeneity similarity reaches an impressive 0.988 (the heatmap of label–label connection frequencies is almost identical for original vs. synthetic), indicating minimal differences in class mixing patterns. These characteristics show that GraphMaster can generate high-quality synthetic graphs that retain key structural properties of the original data. (Additional graph comparison figures are provided in Appendix G.)

4.3 Interpretability Analysis (RQ3)

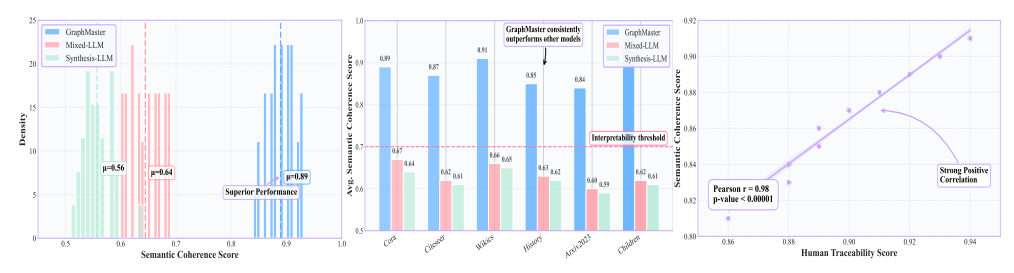
To evaluate the transparency of our GraphMaster model, we conduct both human-centered and algorithmic assessments of interpretability (theoretical details in Appendix H). For human evaluation, 50 expert reviewers rated 200 synthesis instances across three dimensions: process transparency, decision justification, and outcome predictability. The overall Traceability Score quantifies how well humans understand the generation process:

$$T_{\text{score}} = \frac{1}{R \cdot N} \sum_{r=1}^{R} \sum_{i=1}^{N} t_{r,i},$$
(15)

where $t_{r,i}$ represents the score given by reviewer r for instance i. In parallel, we leverage a Grassmann manifold-based approach to systematically assess semantic consistency of synthesized nodes. This mathematical framework provides a principled way to measure how well generated nodes align with the semantic direction of background knowledge, yielding coherence scores in the range [0,1].

Our human evaluation results demonstrate that GraphMaster exhibits excellent interpretability, with an average traceability score of $T_{\rm score} = 0.92$, significantly outperforming Mixed-LLM (0.66) and Synthesis-LLM (0.59). For the Grassmann manifold-based evaluation method, Figure 3a shows that GraphMaster significantly outperforms comparative methods in terms of semantic coherence,

⁴Case study are given in Appendix K.



(a) Semantic Score Distribution (b) Cross-Dataset Comparison (c) Human-Algorithm Agreement

Figure 3: Interpretability Analysis of GraphMaster.

indicating that GraphMaster can generate nodes highly aligned with the principal semantic direction. The score distribution more concentrated in higher value regions also indicates stronger consistency in the quality of generated nodes. Figure 3b shows that GraphMaster maintains high performance across all datasets, consistently exceeding the interpretability threshold of 0.7. Figure 3c demonstrates a strong correlation between human ratings and semantic coherence scores (r=0.78, p<0.00001), further validating our Grassmann manifold-based approach as an effective metric for measuring interpretability. This alignment between human judgment and geometric measures confirms the practical relevance and feasibility of our mathematical framework.

4.4 Ablation Study (RQ4)

Table 2: Ablation experiment in GCN model.

In this section, we investigate the relative importance of various components within the GraphMaster framework and their impact on synthesis quality. We systematically analyze how different agent configurations affect the overall performance. We selected Qwen-32B [1], Deepseek-R1-32B [5] and Llama-33B [4], three models with parameters around 32B, as comparison models. Additionally, we examine how varying the size of the background knowledge base $(N=|\mathcal{K}|)$ and the percentage of newly generated nodes (M%) influences synthesis effectiveness. We trained the model using GCN on six datasets, and the results are presented in Table 2. Our findings indicate that the performance varies significantly across different LLMs, with QwQ-32B consistently outperforming the alternatives by 1.5-2.3% across all datasets. Notably, DeepSeek-R1-32B achieves the second-best performance despite LLaMA-33B having more parameters, suggesting that model architecture and pre-training approach are more critical than raw parameter count for this task.

The ablation results reveal that removing either the Perception Agent or Evaluation Agent substantially degrades performance (by 5.2% and 4.1% on average, respectively), with the Perception Agent proving particularly crucial. This confirms that both specialized components play essential roles in maintaining generation quality and cannot be omitted from the framework. Regarding hyperparameters, we observe that N=30 consistently outperforms both smaller (N=20) and larger (N=40) knowledge bases across all datasets. Similarly, setting M=15% yields optimal results compared to both M=10% and M=20%. These findings demonstrate that while sufficient context is necessary for high-quality synthesis, excessive background knowledge can dilute the model's focus. Likewise, generating too many nodes simultaneously reduces overall quality due to limitations in the model's generative capacity when handling multiple interdependent elements.

5 Conclusion

In this paper, we introduced GraphMaster, the first multi-agent framework for text-attributed graph synthesis that successfully addresses the critical bottleneck of data scarcity in training GFMs. By orchestrating specialized LLM agents in a hierarchical RAG paradigm, our approach systematically overcomes the limitations of traditional synthesis methods, generating semantically rich and structurally coherent graph extensions even in severely data-constrained environments. Beyond the framework itself, we created specialized data-limited variants of six standard graph benchmarks and developed a novel dual-perspective interpretability assessment methodology that combines expert human evaluation with a theoretically grounded Grassmannian manifold-based analysis. Comprehensive experiments demonstrate GraphMaster's consistently superior performance across diverse datasets and downstream GNN architectures. Future work could explore multi-scale synthesis approaches that simultaneously model global topology and local semantics, knowledge transfer mechanisms from data-rich to data-limited domains, and adaptive sampling strategies optimized specifically for synthesis objectives. This work not only provides an immediate solution to the graph data scarcity problem but also establishes foundational methodologies for advancing interpretable graph data synthesis.

6 Acknowledgements

This work is supported by the NSFC Grants U2241211, 62427808 and U24A20255.

References

- [1] Jinze Bai, Shuai Bai, Yunfei Chu, Zeyu Cui, Kai Dang, Xiaodong Deng, Yang Fan, Wenbin Ge, Yu Han, Fei Huang, Binyuan Hui, Luo Ji, Mei Li, Junyang Lin, Runji Lin, Dayiheng Liu, Gao Liu, Chengqiang Lu, Keming Lu, Jianxin Ma, Rui Men, Xingzhang Ren, Xuancheng Ren, Chuanqi Tan, Sinan Tan, Jianhong Tu, Peng Wang, Shijie Wang, Wei Wang, Shengguang Wu, Benfeng Xu, Jin Xu, An Yang, Hao Yang, Jian Yang, Shusheng Yang, Yang Yao, Bowen Yu, Hongyi Yuan, Zheng Yuan, Jianwei Zhang, Xingxuan Zhang, Yichang Zhang, Zhenru Zhang, Chang Zhou, Jingren Zhou, Xiaohuan Zhou, and Tianhang Zhu. Qwen technical report. *arXiv* preprint arXiv:2309.16609, 2023.
- [2] Zekai Chen, Xunkai Li, Yinlin Zhu, Rong-Hua Li, and Guoren Wang. Rethinking client-oriented federated graph learning. In *Proceedings of the 34th ACM International Conference on Information and Knowledge Management (CIKM '25)*, Seoul, Republic of Korea, 2025. ACM.
- [3] Yung-Sung Chuang, Linlu Qiu, Cheng-Yu Hsieh, Ranjay Krishna, Yoon Kim, and James Glass. Lookback lens: Detecting and mitigating contextual hallucinations in large language models using only attention maps. *arXiv* preprint arXiv:2407.07071, 2024.
- [4] Cognitive Computations. Samantha: A sentient ai assistant trained in philosophy, psychology, and personal relationships, 2024. https://huggingface.co/cognitivecomputations/samantha-1.1-llama-33b.
- [5] DeepSeek-AI. Deepseek-r1: Incentivizing reasoning capability in llms via reinforcement learning, 2025.
- [6] Yuhao Deng, Yu Wang, Lei Cao, Lianpeng Qiao, Yuping Wang, Jingzhe Xu, Yizhou Yan, and Samuel Madden. Outlier summarization via human interpretable rules. *Proc. VLDB Endow.*, 17(7):1591–1604, March 2024.
- [7] Kaize Ding, Zhe Xu, Hanghang Tong, and Huan Liu. Data augmentation for deep graph learning: A survey. *SIGKDD Explorations*, 24(2):61–79, 2023.
- [8] Vijay Prakash Dwivedi, Chaitanya K Joshi, Anh Tuan Luu, Thomas Laurent, Yoshua Bengio, and Xavier Bresson. Benchmarking graph neural networks. *arXiv preprint arXiv:2003.00982*, 2020.
- [9] Yushi Feng, Tsai Hor Chan, Guosheng Yin, and Lequan Yu. Democratizing large language model-based graph data augmentation via latent knowledge graphs. *arXiv preprint arXiv:2502.13535*, 2025.
- [10] Jingtong Gao, Xiangyu Zhao, Bo Chen, Fan Yan, Huifeng Guo, and Ruiming Tang. Autotransfer: Instance transfer for cross-domain recommendations. In *Proceedings of the 46th International ACM SIGIR Conference on Research and Development in Information Retrieval (SIGIR '23)*, pages 1478–1487. ACM, 2023.
- [11] C. Lee Giles, Kurt Bollacker, and Steve Lawrence. Citeseer: An automatic citation indexing system. In *Proceedings of the Third ACM Conference on Digital Libraries*, pages 89–98, 1998.
- [12] Zirui Guo, Lianghao Xia, Yanhua Yu, Yuling Wang, Zixuan Yang, Wei Wei, Liang Pang, Tat-Seng Chua, and Chao Huang. Graphedit: Large language models for graph structure learning. In *Arxiv:* 2402.15183, 2025. Preprint available at https://github.com/HKUDS/GraphEdit.
- [13] William L. Hamilton, Zhitao Ying, and Jure Leskovec. Inductive representation learning on large graphs. In *Advances in Neural Information Processing Systems (NeurIPS)*, 2017.
- [14] Xiaotian Han, Zhimeng Jiang, Ninghao Liu, and Xia Hu. G-mixup: Graph data augmentation for graph classification. In *Proceedings of the 39th International Conference on Machine Learning (ICML)*, volume 162, pages 8866–8882. PMLR, 2022.
- [15] Ziniu Hu, Yuxiao Dong, Kuansan Wang, Kai-Wei Chang, and Yizhou Sun. Gpt-gnn: Generative pre-training of graph neural networks. In *Proceedings of the 26th ACM SIGKDD International* Conference on Knowledge Discovery & Data Mining (KDD '20), pages 1857–1867. ACM, 2020.

- [16] Jiarui Ji, Runlin Lei, Jialing Bi, Zhewei Wei, Xu Chen, Yankai Lin, Xuchen Pan, Yaliang Li, and Bolin Ding. LLM-Based Multi-Agent Systems are Scalable Graph Generative Models. arXiv preprint arXiv:2410.09824, 2025.
- [17] Jiarui Ji, Runlin Lei, Jialing Bi, Zhewei Wei, Xu Chen, Yankai Lin, Xuchen Pan, Yaliang Li, and Bolin Ding. Llm-based multi-agent systems are scalable graph generative models. *arXiv* preprint arXiv:2410.09824, 2025.
- [18] Thomas N. Kipf and Max Welling. Semi-supervised classification with graph convolutional networks. In *International Conference on Learning Representations (ICLR)*, 2017.
- [19] Xinye Li, Zunwen Zheng, Qian Zhang, Dekai Zhuang, Jiabao Kang, Liyan Xu, Qingbin Liu, Xi Chen, Zhiying Tu, Dianhui Chu, and Dianbo Sui. Scedit: Script-based assessment of knowledge editing. *arXiv preprint arXiv:2505.23291*, may 2025. A preprint.
- [20] Xunkai Li, Zhengyu Wu, Jiayi Wu, Hanwen Cui, Jishuo Jia, Rong-Hua Li, and Guoren Wang. Graph learning in the era of llms: A survey from the perspective of data, models, and tasks. *arXiv preprint arXiv:2412.12456*, 2024.
- [21] Xunkai Li, Zhengyu Wu, Kaichi Yu, Hongchao Qin, Guang Zeng, Rong-Hua Li, and Guoren Wang. Toward data-centric directed graph learning: An entropy-driven approach. *arXiv preprint arXiv:2505.00983*, 2025. Accepted by ICML 2025.
- [22] Dugang Liu, Chaohua Yang, Xing Tang, Yejing Wang, Fuyuan Lyu, Weihong Luo, Xiuqiang He, Zhong Ming, and Xiangyu Zhao. Multifs: Automated multi-scenario feature selection in deep recommender systems. In *Proceedings of the 17th ACM International Conference on Web Search and Data Mining (WSDM '24)*, pages 434–442. ACM, 2024.
- [23] Jiawei Liu, Cheng Yang, Zhiyuan Lu, Junze Chen, Yibo Li, Mengmei Zhang, Ting Bai, Yuan Fang, Lichao Sun, Philip S. Yu, and Chuan Shi. Graph foundation models: Concepts, opportunities and challenges. *IEEE Transactions on Pattern Analysis and Machine Intelligence*, 2024. Preprint version available on arXiv.
- [24] Guangquan Lu, Wanxin Chen, Yadan Han, Jiamin Tang, and Faliang Huang. Joint graph augmentation and adaptive synthetic sampling for imbalanced node classification. In *Natural Language Processing and Chinese Computing*, 2025.
- [25] Weigang Lu, Ziyu Guan, Wei Zhao, Yaming Yang, Yibing Zhan, Yiheng Lu, and Dapeng Tao. Agmixup: Adaptive graph mixup for semi-supervised node classification. In *Association for the Advancement of Artificial Intelligence (AAAI)*, 2025. Preprint available at https://github.com/WeigangLu/AGMixup.
- [26] Haitao Mao, Zhikai Chen, Wenzhuo Tang, Jianan Zhao, Yao Ma, Tong Zhao, Neil Shah, Mikhail Galkin, and Jiliang Tang. Position: Graph foundation models are already here. arXiv preprint arXiv:2402.02216, 2024. Version 3, revised on 30 May 2024.
- [27] Andrew McCallum, Kamal Nigam, et al. Automating the construction of internet portals with machine learning. In *Proceedings of the Seventh International Conference on Machine Learning*, pages 79–86, 2000.
- [28] Nick McKenna, Tianyi Li, Liang Cheng, Mohammad Javad Hosseini, Mark Johnson, and Mark Steedman. Sources of hallucination by large language models on inference tasks. *arXiv* preprint *arXiv*:2305.14552, 2023.
- [29] Xuchen Pan, Dawei Gao, Yuexiang Xie, Yushuo Chen, Zhewei Wei, Yaliang Li, and Bolin Ding. Very Large-Scale Multi-Agent Simulation in AgentScope. arXiv preprint arXiv:2407.17789, 2024.
- [30] Nils Reimers and Iryna Gurevych. Sentence-bert: Sentence embeddings using siamese BERT-networks. In *Proceedings of the 2019 Conference on Empirical Methods in Natural Language Processing (EMNLP)*, Hong Kong, China, 2019. Association for Computational Linguistics.

- [31] Laurent Rigoux, Xavier Brown, Thomas Laurent, Adam Predel, Yann LeCun, and Bryan Hooi. Harnessing explanations: Llm-to-lm interpreter for enhanced text-attributed graph representation learning. In *Proceedings of the International Conference on Learning Representations (ICLR)*, 2024. arXiv:2013.105235v5 [cs.LG].
- [32] Qwen Team. Qwq-32b: Embracing the power of reinforcement learning, March 2025.
- [33] Petar Velicković, Guillem Cucurull, Arantxa Casanova, Adriana Romero, Pietro Lio, and Yoshua Bengio. Graph attention networks. In *International Conference on Learning Representations* (*ICLR*), 2018.
- [34] Vikas Verma, Alex Lamb, Christopher Beckham, Amir Najafi, Ioannis Mitliagkas, David Lopez-Paz, and Yoshua Bengio. Manifold mixup: Better representations by interpolating hidden states. In *Proceedings of the 36th International Conference on Machine Learning (ICML)*, pages 6438–6447. PMLR, 2019.
- [35] Yiwei Wang, Wei Wang, Yuxuan Liang, Yujun Cai, Juncheng Liu, and Bryan Hooi. Nodeaug: Semi-supervised node classification with data augmentation. In *Proceedings of the 26th ACM SIGKDD Conference on Knowledge Discovery and Data Mining (KDD)*, pages 207–217. ACM, 2020.
- [36] Yizhong Wang, Yeganeh Kordi, Swaroop Mishra, Alisa Liu, Noah A. Smith, Daniel Khashabi, and Hannaneh Hajishirzi. SELF-INSTRUCT: Aligning language models with self-generated instructions. arXiv preprint arXiv:2212.10560, 2023.
- [37] Zichong Wang, Zhipeng Yin, Yuying Zhang, Liping Yang, Tingting Zhang, Niki Pissinou, Yu Cai, Shu Hu, Yun Li, Liang Zhao, and Wenbin Zhang. Fg-smote: Towards fair node classification with graph neural network. In *SIGKDD Explorations*, 2025.
- [38] Yanzhe Wen, Xunkai Li, Qi Zhang, Zhu Lei, Guang Zeng, Rong-Hua Li, and Guoren Wang. When llms meet open-world graph learning: A new perspective for unlabeled data uncertainty. *arXiv preprint arXiv:2505.13989*, 2025.
- [39] Xiang Wu, Xunkai Li, Rong-Hua Li, Kangfei Zhao, and Guoren Wang. Scadyg: A new paradigm for large-scale dynamic graph learning. *arXiv preprint arXiv:2501.16002*, 2025.
- [40] Zhengyu Wu, Xunkai Li, Yinlin Zhu, Rong-Hua Li, Guoren Wang, and Chenghu Zhou. Federated prototype graph learning. *arXiv preprint arXiv:2504.09493*, 2025.
- [41] Keyulu Xu, Weihua Hu, Jure Leskovec, and Stefanie Jegelka. Jumping knowledge networks. In *International Conference on Learning Representations (ICLR)*, 2018.
- [42] Yao Xu, Shizhu He, Jiabei Chen, et al. Generate-on-Graph: Treat llm as both agent and kg for incomplete knowledge graph question answering. arXiv preprint arXiv:2404.14741, 2024.
- [43] Hao Yan, Chaozhuo Li, Ruosong Long, Chao Yan, Jianan Zhao, Wenwen Zhuang, Jun Yin, Peiyan Zhang, Weihao Han, Hao Sun, et al. A comprehensive study on text-attributed graphs: Benchmarking and rethinking. *Advances in Neural Information Processing Systems*, 36:17238–17264, 2023.
- [44] Fuda Ye, Shuangyin Li, Yongqi Zhang, and Lei Chen. R²AG: Incorporating retrieval information into retrieval augmented generation. In Yaser Al-Onaizan, Mohit Bansal, and Yun-Nung Chen, editors, *Findings of the Association for Computational Linguistics: EMNLP 2024*, pages 11584–11596, Miami, Florida, USA, November 2024. Association for Computational Linguistics.
- [45] Jianxiang Yu, Yuxiang Ren, Chenghua Gong, Jiaqi Tan, Xiang Li, and Xuecang Zhang. Leveraging large language models for node generation in few-shot learning on text-attributed graphs. In *Proceedings of the AAAI Conference on Artificial Intelligence*. Association for the Advancement of Artificial Intelligence, 2025.
- [46] Hao Zhang, Xunkai Li, Yinlin Zhu, and Lianglin Hu. Rethinking federated graph learning: A data condensation perspective. In *Proceedings of the Thirty-Fourth International Joint Conference on Artificial Intelligence (IJCAI-25)*, 2025.

- [47] Hongyi Zhang, Moustapha Cisse, Yann N Dauphin, and David Lopez-Paz. mixup: Beyond empirical risk minimization. In *International Conference on Learning Representations (ICLR)*, 2018.
- [48] Qinggang Zhang, Shengyuan Chen, Yuanchen Bei, Zheng Yuan, Huachi Zhou, Zijin Hong, Junnan Dong, Hao Chen, Yi Chang, and Xiao Huang. A survey of graph retrieval-augmented generation for customized large language models. arXiv preprint arXiv:2501.13958, 2025.
- [49] Yongqi Zhang and Quanming Yao. Knowledge graph reasoning with relational digraph. *arXiv* preprint, 2021. Preprint.
- [50] Yongqi Zhang, Quanming Yao, Ling Yue, Xian Wu, Ziheng Zhang, Zhenxi Lin, and Yefeng Zheng. Emerging drug interaction prediction enabled by flow-based graph neural network with biomedical network. *arXiv preprint*, 2023. Preprint.
- [51] Yongqi Zhang, Zhanke Zhou, Quanming Yao, Xiaowen Chu, and Bo Han. Adaprop: Learning adaptive propagation for graph neural network based knowledge graph reasoning. In *Proceedings of the 29th ACM SIGKDD Conference on Knowledge Discovery and Data Mining (KDD '23)*, Long Beach, CA, USA, 2023.
- [52] Yongqi Zhang, Zhanke Zhou, Quanming Yao, and Yong Li. Efficient hyper-parameter search for knowledge graph embedding. In *Proceedings of the 60th Annual Meeting of the Association* for Computational Linguistics (Volume 1: Long Papers), pages 2715–2735, Dublin, Ireland, May 2022. Association for Computational Linguistics.
- [53] Zhihan Zhang, Xunkai Li, Zhu Lei, Guang Zeng, Ronghua Li, and Guoren Wang. Rethinking graph structure learning in the era of llms. *arXiv preprint arXiv:2503.21223*, 2025.
- [54] Zhongjian Zhang, Xiao Wang, Huichi Zhou, Yue Yu, Mengmei Zhang, Cheng Yang, and Chuan Shi. Can large language models improve the adversarial robustness of graph neural networks? In *Proceedings of the 31st ACM SIGKDD Conference on Knowledge Discovery and Data Mining (KDD '25)*, pages 1–14, 2025.
- [55] Zihao Zhang, Xunkai Li, Rong-Hua Li, Bing Zhou, Zhenjun Li, and Guoren Wang. Toward general and robust llm-enhanced text-attributed graph learning. arXiv preprint arXiv:2504.02343, 2025.
- [56] Tianxiang Zhao, Xiang Zhang, and Suhang Wang. Graphsmote: Imbalanced node classification on graphs with graph neural networks. In *Proceedings of the Fourteenth ACM International Conference on Web Search and Data Mining (WSDM)*, pages 833–841. ACM, 2021.
- [57] Tong Zhao, Yozen Liu, Leonardo Neves, Oliver Woodford, Meng Jiang, and Neil Shah. Data augmentation for graph neural networks. In *Proceedings of the AAAI Conference on Artificial Intelligence*, volume 35, pages 11015–11023, 2021.
- [58] Shenghe Zheng, Hongzhi Wang, and Xianglong Liu. Intramix: Intra-class mixup generation for accurate labels and neighbors, 2024. Accepted by NeurIPS2024.
- [59] Jiajun Zhou, Jie Shen, and Qi Xuan. Data augmentation for graph classification. In Proceedings of the 29th ACM International Conference on Information and Knowledge Management (CIKM '20), pages 2341–2348. ACM, 2020.
- [60] Yinlin Zhu, Xunkai Li, Jishuo Jia, Miao Hu, Di Wu, and Meikang Qiu. Towards effective federated graph foundation model via mitigating knowledge entanglement. arXiv preprint arXiv:2505.12684, 2025.

NeurIPS Paper Checklist

1. Claims

Question: Do the main claims made in the abstract and introduction accurately reflect the paper's contributions and scope?

Answer: [Yes]

Justification: In the abstract and introduction, we described in detail the applicable scenario of our model - text attribute graph data synthesis based on a large language model. We also emphasized our contribution - the first RAG-based multi-agent TAG synthesis method, and proposed a new data-limited datasets and a manual and Grassmann Manifold-based semantic dual-view interpretability evaluation method. This is a fundamental breakthrough for the development of this direction.

Guidelines:

- The answer NA means that the abstract and introduction do not include the claims made in the paper.
- The abstract and/or introduction should clearly state the claims made, including the contributions made in the paper and important assumptions and limitations. A No or NA answer to this question will not be perceived well by the reviewers.
- The claims made should match theoretical and experimental results, and reflect how much the results can be expected to generalize to other settings.
- It is fine to include aspirational goals as motivation as long as it is clear that these goals are not attained by the paper.

2. Limitations

Question: Does the paper discuss the limitations of the work performed by the authors?

Answer: [Yes]

Justification: See Appendix J.

Guidelines:

- The answer NA means that the paper has no limitation while the answer No means that the paper has limitations, but those are not discussed in the paper.
- The authors are encouraged to create a separate "Limitations" section in their paper.
- The paper should point out any strong assumptions and how robust the results are to violations of these assumptions (e.g., independence assumptions, noiseless settings, model well-specification, asymptotic approximations only holding locally). The authors should reflect on how these assumptions might be violated in practice and what the implications would be.
- The authors should reflect on the scope of the claims made, e.g., if the approach was only tested on a few datasets or with a few runs. In general, empirical results often depend on implicit assumptions, which should be articulated.
- The authors should reflect on the factors that influence the performance of the approach. For example, a facial recognition algorithm may perform poorly when image resolution is low or images are taken in low lighting. Or a speech-to-text system might not be used reliably to provide closed captions for online lectures because it fails to handle technical jargon.
- The authors should discuss the computational efficiency of the proposed algorithms and how they scale with dataset size.
- If applicable, the authors should discuss possible limitations of their approach to address problems of privacy and fairness.
- While the authors might fear that complete honesty about limitations might be used by reviewers as grounds for rejection, a worse outcome might be that reviewers discover limitations that aren't acknowledged in the paper. The authors should use their best judgment and recognize that individual actions in favor of transparency play an important role in developing norms that preserve the integrity of the community. Reviewers will be specifically instructed to not penalize honesty concerning limitations.

3. Theory assumptions and proofs

Question: For each theoretical result, does the paper provide the full set of assumptions and a complete (and correct) proof?

Answer: [Yes]

Justification: We prove in detail in Appendix I that GraphMaster can synthesize TAG data with consistent semantics and structure, and propose in detail the theoretical theorem and corresponding proofs on interpretable experiments in Appendix H.

Guidelines:

- The answer NA means that the paper does not include theoretical results.
- All the theorems, formulas, and proofs in the paper should be numbered and cross-referenced.
- All assumptions should be clearly stated or referenced in the statement of any theorems.
- The proofs can either appear in the main paper or the supplemental material, but if they appear in the supplemental material, the authors are encouraged to provide a short proof sketch to provide intuition.
- Inversely, any informal proof provided in the core of the paper should be complemented by formal proofs provided in appendix or supplemental material.
- Theorems and Lemmas that the proof relies upon should be properly referenced.

4. Experimental result reproducibility

Question: Does the paper fully disclose all the information needed to reproduce the main experimental results of the paper to the extent that it affects the main claims and/or conclusions of the paper (regardless of whether the code and data are provided or not)?

Answer: [Yes]

Justification: We have described in detail the principles of our model GraphMaster, as well as the experimental parameters, hardware configuration, and specific experimental methods. At the same time, we also provide the specific creation algorithm for the data-limited dataset and the specific principles, parameter configuration, and hardware configuration of two self-created LLM-based baselines. We believe that we have filled in all the details and promise to open source all the codes and datasets after the paper is accepted.

Guidelines:

- The answer NA means that the paper does not include experiments.
- If the paper includes experiments, a No answer to this question will not be perceived well by the reviewers: Making the paper reproducible is important, regardless of whether the code and data are provided or not.
- If the contribution is a dataset and/or model, the authors should describe the steps taken to make their results reproducible or verifiable.
- Depending on the contribution, reproducibility can be accomplished in various ways. For example, if the contribution is a novel architecture, describing the architecture fully might suffice, or if the contribution is a specific model and empirical evaluation, it may be necessary to either make it possible for others to replicate the model with the same dataset, or provide access to the model. In general, releasing code and data is often one good way to accomplish this, but reproducibility can also be provided via detailed instructions for how to replicate the results, access to a hosted model (e.g., in the case of a large language model), releasing of a model checkpoint, or other means that are appropriate to the research performed.
- While NeurIPS does not require releasing code, the conference does require all submissions to provide some reasonable avenue for reproducibility, which may depend on the nature of the contribution. For example
 - (a) If the contribution is primarily a new algorithm, the paper should make it clear how to reproduce that algorithm.
 - (b) If the contribution is primarily a new model architecture, the paper should describe the architecture clearly and fully.
 - (c) If the contribution is a new model (e.g., a large language model), then there should either be a way to access this model for reproducing the results or a way to reproduce the model (e.g., with an open-source dataset or instructions for how to construct the dataset).

(d) We recognize that reproducibility may be tricky in some cases, in which case authors are welcome to describe the particular way they provide for reproducibility. In the case of closed-source models, it may be that access to the model is limited in some way (e.g., to registered users), but it should be possible for other researchers to have some path to reproducing or verifying the results.

5. Open access to data and code

Question: Does the paper provide open access to the data and code, with sufficient instructions to faithfully reproduce the main experimental results, as described in supplemental material?

Answer: [Yes]

Justification: After the paper is accepted, we will open source the complete data-limited dataset and its creation code, the self-created code for the LLM-based baseline, and the detailed code of GraphMaster. We have submitted the GraphMaster code at this stage, but we believe it can still be improved. We will further optimize it in subsequent versions to ensure that it is plug-and-play and has a clear structure. You can find the code in Appendix ??.

Guidelines:

- The answer NA means that paper does not include experiments requiring code.
- Please see the NeurIPS code and data submission guidelines (https://nips.cc/public/guides/CodeSubmissionPolicy) for more details.
- While we encourage the release of code and data, we understand that this might not be possible, so "No" is an acceptable answer. Papers cannot be rejected simply for not including code, unless this is central to the contribution (e.g., for a new open-source benchmark).
- The instructions should contain the exact command and environment needed to run to reproduce the results. See the NeurIPS code and data submission guidelines (https://nips.cc/public/guides/CodeSubmissionPolicy) for more details.
- The authors should provide instructions on data access and preparation, including how to access the raw data, preprocessed data, intermediate data, and generated data, etc.
- The authors should provide scripts to reproduce all experimental results for the new proposed method and baselines. If only a subset of experiments are reproducible, they should state which ones are omitted from the script and why.
- At submission time, to preserve anonymity, the authors should release anonymized versions (if applicable).
- Providing as much information as possible in supplemental material (appended to the paper) is recommended, but including URLs to data and code is permitted.

6. Experimental setting/details

Question: Does the paper specify all the training and test details (e.g., data splits, hyper-parameters, how they were chosen, type of optimizer, etc.) necessary to understand the results?

Answer: [Yes]

Justification: Our paper contains all the training and testing details. Even if there is something that is not mentioned in the paper (although we have checked many times, it is not impossible), you can still find the corresponding answer through the code.

Guidelines:

- The answer NA means that the paper does not include experiments.
- The experimental setting should be presented in the core of the paper to a level of detail that is necessary to appreciate the results and make sense of them.
- The full details can be provided either with the code, in appendix, or as supplemental
 material.

7. Experiment statistical significance

Question: Does the paper report error bars suitably and correctly defined or other appropriate information about the statistical significance of the experiments?

Answer: [Yes]

Justification: We included error bars in both the main experiment and the ablation experiment - as mentioned in the main text. To ensure the robustness of our experiments, we repeated each experiment 50 times and reported the mean and standard deviation of the results. At the same time, for the interpretability analysis, we also performed multiple experiments (selecting multiple reviewers for averaging) to ensure the correctness of the experimental results.

Guidelines:

- The answer NA means that the paper does not include experiments.
- The authors should answer "Yes" if the results are accompanied by error bars, confidence intervals, or statistical significance tests, at least for the experiments that support the main claims of the paper.
- The factors of variability that the error bars are capturing should be clearly stated (for example, train/test split, initialization, random drawing of some parameter, or overall run with given experimental conditions).
- The method for calculating the error bars should be explained (closed form formula, call to a library function, bootstrap, etc.)
- The assumptions made should be given (e.g., Normally distributed errors).
- It should be clear whether the error bar is the standard deviation or the standard error
 of the mean.
- It is OK to report 1-sigma error bars, but one should state it. The authors should preferably report a 2-sigma error bar than state that they have a 96% CI, if the hypothesis of Normality of errors is not verified.
- For asymmetric distributions, the authors should be careful not to show in tables or figures symmetric error bars that would yield results that are out of range (e.g. negative error rates).
- If error bars are reported in tables or plots, The authors should explain in the text how they were calculated and reference the corresponding figures or tables in the text.

8. Experiments compute resources

Question: For each experiment, does the paper provide sufficient information on the computer resources (type of compute workers, memory, time of execution) needed to reproduce the experiments?

Answer: [Yes]

Justification: We present parameter configuration and estimated resources in detail.

Guidelines:

- The answer NA means that the paper does not include experiments.
- The paper should indicate the type of compute workers CPU or GPU, internal cluster, or cloud provider, including relevant memory and storage.
- The paper should provide the amount of compute required for each of the individual experimental runs as well as estimate the total compute.
- The paper should disclose whether the full research project required more compute than the experiments reported in the paper (e.g., preliminary or failed experiments that didn't make it into the paper).

9. Code of ethics

Question: Does the research conducted in the paper conform, in every respect, with the NeurIPS Code of Ethics https://neurips.cc/public/EthicsGuidelines?

Answer: [Yes]

Justification: We carefully reviewed the Code of Ethics and are confident that we are in compliance.

Guidelines:

• The answer NA means that the authors have not reviewed the NeurIPS Code of Ethics.

- If the authors answer No, they should explain the special circumstances that require a
 deviation from the Code of Ethics.
- The authors should make sure to preserve anonymity (e.g., if there is a special consideration due to laws or regulations in their jurisdiction).

10. Broader impacts

Question: Does the paper discuss both potential positive societal impacts and negative societal impacts of the work performed?

Answer: [Yes]

Justification: We discussed the possible impact of our work on the community - because our work is groundbreaking, proposes new benchmark datasets and evaluation methods, and provides two baselines, and most importantly, proposes a sota method - GraphMaster, which we believe will have a very positive impact on the community and society.

Guidelines:

- The answer NA means that there is no societal impact of the work performed.
- If the authors answer NA or No, they should explain why their work has no societal impact or why the paper does not address societal impact.
- Examples of negative societal impacts include potential malicious or unintended uses (e.g., disinformation, generating fake profiles, surveillance), fairness considerations (e.g., deployment of technologies that could make decisions that unfairly impact specific groups), privacy considerations, and security considerations.
- The conference expects that many papers will be foundational research and not tied to particular applications, let alone deployments. However, if there is a direct path to any negative applications, the authors should point it out. For example, it is legitimate to point out that an improvement in the quality of generative models could be used to generate deepfakes for disinformation. On the other hand, it is not needed to point out that a generic algorithm for optimizing neural networks could enable people to train models that generate Deepfakes faster.
- The authors should consider possible harms that could arise when the technology is being used as intended and functioning correctly, harms that could arise when the technology is being used as intended but gives incorrect results, and harms following from (intentional or unintentional) misuse of the technology.
- If there are negative societal impacts, the authors could also discuss possible mitigation strategies (e.g., gated release of models, providing defenses in addition to attacks, mechanisms for monitoring misuse, mechanisms to monitor how a system learns from feedback over time, improving the efficiency and accessibility of ML).

11. Safeguards

Question: Does the paper describe safeguards that have been put in place for responsible release of data or models that have a high risk for misuse (e.g., pretrained language models, image generators, or scraped datasets)?

Answer: [NA]

Justification: Our paper does not apply to this part.

Guidelines:

- The answer NA means that the paper poses no such risks.
- Released models that have a high risk for misuse or dual-use should be released with
 necessary safeguards to allow for controlled use of the model, for example by requiring
 that users adhere to usage guidelines or restrictions to access the model or implementing
 safety filters.
- Datasets that have been scraped from the Internet could pose safety risks. The authors should describe how they avoided releasing unsafe images.
- We recognize that providing effective safeguards is challenging, and many papers do
 not require this, but we encourage authors to take this into account and make a best
 faith effort.

12. Licenses for existing assets

Question: Are the creators or original owners of assets (e.g., code, data, models), used in the paper, properly credited and are the license and terms of use explicitly mentioned and properly respected?

Answer: [Yes]

Justification: The datasets and baselines we use are cited in detail and ensure that they are open source and allowed for academic use.

Guidelines:

- The answer NA means that the paper does not use existing assets.
- The authors should cite the original paper that produced the code package or dataset.
- The authors should state which version of the asset is used and, if possible, include a URL.
- The name of the license (e.g., CC-BY 4.0) should be included for each asset.
- For scraped data from a particular source (e.g., website), the copyright and terms of service of that source should be provided.
- If assets are released, the license, copyright information, and terms of use in the package should be provided. For popular datasets, paperswithcode.com/datasets has curated licenses for some datasets. Their licensing guide can help determine the license of a dataset.
- For existing datasets that are re-packaged, both the original license and the license of the derived asset (if it has changed) should be provided.
- If this information is not available online, the authors are encouraged to reach out to the asset's creators.

13. New assets

Question: Are new assets introduced in the paper well documented and is the documentation provided alongside the assets?

Answer: [Yes]

Justification: We introduce a new dataset and present the detailed method for creating it.

Guidelines:

- The answer NA means that the paper does not release new assets.
- Researchers should communicate the details of the dataset/code/model as part of their submissions via structured templates. This includes details about training, license, limitations, etc.
- The paper should discuss whether and how consent was obtained from people whose asset is used.
- At submission time, remember to anonymize your assets (if applicable). You can either create an anonymized URL or include an anonymized zip file.

14. Crowdsourcing and research with human subjects

Question: For crowdsourcing experiments and research with human subjects, does the paper include the full text of instructions given to participants and screenshots, if applicable, as well as details about compensation (if any)?

Answer: [Yes]

Justification: In our explainability experiment, we invited 50 computer experts to evaluate the explainability of the model-generated content and compensated them in accordance with our local regulations (due to anonymity and local regulatory restrictions, we are unable to provide compensation details and screenshots).

Guidelines:

- The answer NA means that the paper does not involve crowdsourcing nor research with human subjects.
- Including this information in the supplemental material is fine, but if the main contribution of the paper involves human subjects, then as much detail as possible should be included in the main paper.

 According to the NeurIPS Code of Ethics, workers involved in data collection, curation, or other labor should be paid at least the minimum wage in the country of the data collector.

15. Institutional review board (IRB) approvals or equivalent for research with human subjects

Question: Does the paper describe potential risks incurred by study participants, whether such risks were disclosed to the subjects, and whether Institutional Review Board (IRB) approvals (or an equivalent approval/review based on the requirements of your country or institution) were obtained?

Answer: [NA]

Justification: Our papers do not contain human subjects.

Guidelines:

- The answer NA means that the paper does not involve crowdsourcing nor research with human subjects.
- Depending on the country in which research is conducted, IRB approval (or equivalent)
 may be required for any human subjects research. If you obtained IRB approval, you
 should clearly state this in the paper.
- We recognize that the procedures for this may vary significantly between institutions and locations, and we expect authors to adhere to the NeurIPS Code of Ethics and the guidelines for their institution.
- For initial submissions, do not include any information that would break anonymity (if applicable), such as the institution conducting the review.

16. Declaration of LLM usage

Question: Does the paper describe the usage of LLMs if it is an important, original, or non-standard component of the core methods in this research? Note that if the LLM is used only for writing, editing, or formatting purposes and does not impact the core methodology, scientific rigorousness, or originality of the research, declaration is not required.

Answer: [Yes]

Justification: Our paper explores the use of LLM for TAG data synthesis, and the paper introduces the use of LLM in detail.

Guidelines:

- The answer NA means that the core method development in this research does not involve LLMs as any important, original, or non-standard components.
- Please refer to our LLM policy (https://neurips.cc/Conferences/2025/LLM) for what should or should not be described.

A Comparison of GraphMaster with Recent Representative Works

Recent advancements in leveraging Large Language Models (LLMs) for graph-related tasks have produced several notable approaches. In this section, we conduct a rigorous comparison between our proposed GraphMaster framework and two recent representative works: GAG [17] and LLM4NG [45]. We structure our analysis across three key dimensions: motivation, methodology, and application scenarios, to clearly delineate the unique contributions and advantages of GraphMaster.

A.1 Comparison Between GraphMaster and GAG

A.1.1 Motivation

GraphMaster addresses a fundamental bottleneck in developing Graph Foundation Models (GFMs): the scarcity of large-scale, semantically rich graph datasets. Our work specifically targets the generation of high-quality text-attributed graphs in data-limited environments, focusing on both semantic coherence and structural integrity. In contrast, GAG [17] primarily aims to simulate the dynamic evolution of social graphs through actor-item interactions, with emphasis on reproducing macroscopic network properties such as power-law degree distributions and small-world phenomena. While GAG attempts to capture emergent properties of large-scale social networks, it lacks explicit mechanisms for maintaining semantic coherence in node attributes, which is a critical requirement for training effective GFMs.

A.1.2 Methodology

GraphMaster implements a hierarchical multi-agent framework formalized through the RAG paradigm, where specialized agents perform distinct functions within a closed-loop optimization system:

$$G_{new} = \Psi_{RAG}(G, Q, R, A_{retrieve}, A_{generate}, A_{evaluate})$$
(16)

where G is the original graph, Q represents the query formulation, R denotes the retrieval strategy, and $A_{retrieve}$, $A_{generate}$, and $A_{evaluate}$ correspond to the agent-specific functions. Our Perception Agent extracts knowledge through semantic-enriched modularity maximization:

$$Q_{sem} = \frac{1}{2m} \sum_{i,j} \left[A_{ij} - \gamma \frac{k_i k_j}{2m} - (1 - \gamma) \frac{d_{sem}(x_i, x_j)}{\sum_{l,m} d_{sem}(x_l, x_m)} \right] \delta(c_i, c_j)$$
(17)

In contrast, GAG employs a bipartite graph model where homogeneous "actor" agents interact with items through a retrieval system. Their S-RAG algorithm models actor-item interactions but lacks explicit quality control:

$$p_{ij} = \sigma \left(\theta_1 \cdot sim(x_i, x_j) + \theta_2 \cdot \frac{|N(v_i) \cap N(v_j)|}{|N(v_i)|} + \theta_3 \cdot \frac{k_j}{\max_l k_l} \right)$$
(18)

GraphMaster's multi-agent architecture provides several key advantages: (1) Our Manager Agent dynamically optimizes a multi-objective utility function that balances semantic coherence, structural integrity, and class balance; (2) Our Evaluation Agent implements a comprehensive verification mechanism with adaptive thresholds; and (3) Our theoretical framework provides formal guarantees for information preservation, generation quality, and convergence properties.

A.1.3 Application Scenarios

GraphMaster is explicitly designed for enhancing text-attributed graphs in data-limited environments, making it particularly suitable for academic, industrial, and web-scale applications where data acquisition is costly or restricted. Our framework produces semantically rich and structurally coherent graph extensions that serve as high-quality training data for GFMs. GAG primarily focuses on social network simulation, with applications in modeling online user interactions and social dynamics. While GAG can generate large-scale graphs (up to 100,000 nodes), it sacrifices semantic richness for scale and does not provide guarantees on the quality of textual attributes. Our evaluation framework, combining human assessment with Grassmannian manifold-based analysis, demonstrates that GraphMaster consistently produces higher-quality graph extensions that better preserve both semantic and structural characteristics of the original data.

A.2 Comparison Between GraphMaster and LLM4NG

A.2.1 Motivation

GraphMaster addresses the broad challenge of data scarcity for GFMs through comprehensive graph synthesis that enhances both node attributes and structural properties. In contrast, LLM4NG [45] specifically targets few-shot learning scenarios in node classification, with a narrow focus on enhancing class-level information. While LLM4NG aims to improve classification performance by adding labeled examples, it does not address the fundamental issue of enhancing the overall quality and representational capacity of graph data. GraphMaster's approach is more comprehensive, as it treats the graph synthesis problem holistically, generating high-quality nodes and edges that maintain both semantic and structural coherence.

A.2.2 Methodology

GraphMaster employs a sophisticated multi-agent system with specialized roles and iterative refinement cycles. Our Enhancement Agent generates new nodes through a conditional autoregressive model:

$$P(x_s|K) = \prod_{i=1}^{L} P(x_s^i|x_s^{< i}, X_k, E_k, K)$$
(19)

and models edge connections with a probability function that balances semantic, structural, and degree-based factors:

$$P((v_s, v_i) \in E_c | K) = \sigma \left(\theta_1 \cdot sim(x_s, x_i) + \theta_2 \cdot \frac{|N(v_i) \cap N_K(v_s)|}{|N_K(v_s)|} + \theta_3 \cdot \frac{k_i}{\max_j k_j} \right)$$
(20)

LLM4NG adopts a significantly simpler approach, primarily generating text based on label characteristics alone. Its core idea is to let the large language model generate text that meets class characteristics based solely on the name of the label:

$$s_q = \text{LLM}(\text{Prompt}(c)), c \in C$$
 (21)

followed by a basic edge predictor that often introduces noise and structural inconsistencies:

$$\hat{y}e(h_{v_i}, h_{v_j}) = \text{MLP}(h_{v_i}||h_{v_j})$$
(22)

GraphMaster's methodology offers several crucial advantages: (1) Our approach maintains structural consistency through explicit modeling of node-edge relationships; (2) Our iterative refinement process ensures high-quality synthesis through adaptive thresholds; and (3) Our theoretical framework provides formal guarantees on the quality and convergence of the synthesis process. LLM4NG lacks these quality assurance mechanisms and theoretical foundations.

A.2.3 Application Scenarios

GraphMaster addresses a wider range of data-limited scenarios and can enhance graphs for various downstream tasks beyond classification. Our framework is particularly effective in scenarios requiring high semantic coherence and structural fidelity, such as scientific discovery, knowledge graph completion, and recommendation systems.

LLM4NG is narrowly optimized for classification tasks in few-shot scenarios, with limited impact on the overall graph structure. When applied to data-limited scenarios rather than strictly few-shot learning, LLM4NG's edge generation methods often introduce significant noise and interference to the graph structure. This limitation is evidenced by its poor performance in our experimental evaluations on data-limited datasets. The edge probabilities predicted by its simple model fail to capture the complex structural patterns present in real-world graphs.

While LLM4NG offers computational efficiency through its lightweight design, it sacrifices synthesis quality, broader applicability, and introduces potential structural inconsistencies. Our experimental results demonstrate that GraphMaster achieves superior performance across multiple datasets and tasks, particularly in generating semantically coherent and structurally valid graph extensions that maintain both local and global properties of the original graph.

B The implement details of newly created baseline

B.1 Mixed-LLM

Mixed-LLM introduces a novel interpolative synthesis approach that extends the seminal mixup concept from computer vision to text-attributed graphs via large language models. This method operates on the principle of manifold-aware semantic interpolation, where node representations from different classes are strategically combined to generate semantically coherent yet diverse synthetic nodes.

The Mixed-LLM algorithm consists of three primary phases:

1. **Strategic Class-Balanced Sampling**: Rather than random selection, Mixed-LLM employs a distribution-aware sampling strategy:

$$S = \{(v_i, y_i) | v_i \in V, P(v_i) \propto 1/|V_{y_i}|^{\alpha} \}$$
(23)

where α is an adaptive parameter controlling the emphasis on minority classes and $|V_{y_i}|$ represents the cardinality of nodes with label y_i .

2. Latent Space Interpolation: For each pair of sampled nodes (v_i, v_j) , Mixed-LLM generates a convex combination in the semantic space:

$$\tilde{x}_s = \lambda \cdot \phi_{LLM}(x_i) + (1 - \lambda) \cdot \phi_{LLM}(x_i) \tag{24}$$

where ϕ_{LLM} represents the LLM's latent representation function and $\lambda \sim \text{Beta}(\alpha, \alpha)$ is a mixing coefficient.

3. **LLM-Guided Textual Manifestation**: The interpolated representation is transformed into coherent textual attributes through a prompt-based generation:

$$x_s = \text{LLM}_M(p(\tilde{x}_s, x_i, x_i, y_i, y_i)) \tag{25}$$

where p is a carefully designed prompt template instructing the LLM to create textual attributes that preserve the semantic characteristics of both source nodes while maintaining linguistic naturalness.

The final label assignment follows a soft probability distribution:

$$P(y_s = c) = \lambda \cdot I[y_i = c] + (1 - \lambda) \cdot I[y_i = c]$$
(26)

where I is the indicator function. This probabilistic formulation enables Mixed-LLM to generate boundary-enhancing examples that improve classifier robustness.

B.2 Synthesis-LLM

Synthesis-LLM implements a context-aware graph sampling and generative synthesis framework that leverages structural locality principles to inform LLM-based node generation. Unlike conventional approaches that process graph data indiscriminately, Synthesis-LLM employs sophisticated topological sampling to create representative subgraph contexts that maximize information density within LLM token constraints.

The framework operates in four sequential stages:

1. **Multi-strategy Subgraph Sampling**: Synthesis-LLM employs a hybrid sampling approach that combines Personalized PageRank (PPR) with strategic breadth-first search:

$$K_s = \Gamma_{PPR}(G, v_s, \alpha, r) \cup \Gamma_{BFS}(G, v_s, d)$$
(27)

where Γ_{PPR} samples nodes based on their PPR scores from seed node v_s with damping factor α and threshold r, while Γ_{BFS} complements this with a depth-limited breadth-first expansion to depth d.

2. **Structural-Semantic Context Formulation**: The sampled subgraph is transformed into a rich prompt context:

$$C = f_{context}(K_s, A[K_s], X[K_s])$$
(28)

where $f_{context}$ is a specialized function that encodes both topological relationships and textual attributes into a structured prompt format.

3. **Guided Generative Synthesis**: The LLM generates new nodes conditioned on the extracted context:

$$(x_s, E_s) = LLM_S(C, \theta) \tag{29}$$

where LLM_S represents the synthesis LLM with temperature parameter θ that balances creativity and fidelity.

4. **Structural Consistency Enforcement**: Generated nodes undergo topological validation to ensure adherence to the original graph's structural patterns:

$$E'_{s} = \{ e \in E_{s} | P_{structure}(e|G) > \tau \}$$
(30)

where $P_{structure}$ estimates the probability of edge e existing given the structural patterns in G, and τ is an acceptance threshold.

This methodology enables Synthesis-LLM to generate nodes that maintain both semantic relevance and structural coherence with respect to the original graph, while requiring minimal examples due to the LLM's inherent understanding of semantic relationships.

B.3 Experimental details

We selected QwQ-32B [32] as the large language model for these two baselines, and used two A6000 GPUs with 48G memory for the experiments.

B.3.1 Hyperparameter Selection for Mixed-LLM

In Mixed-LLM, extensive grid search and ablation studies were conducted to optimize key hyperparameters. The class balancing parameter α was tuned within the range [0.5, 1.5] with an optimal value of 0.8, ensuring a good balance between preserving the original class distribution and addressing class imbalance issues. The beta distribution parameter for the mixing coefficient, where $\lambda \sim \text{Beta}(\alpha, \alpha)$, achieved optimal performance at 0.4, producing meaningful boundary examples. Additionally, an LLM temperature of 0.7 provided the best balance between creative variation and semantic consistency, and incorporating 2–3 example interpolations in the prompt significantly enhanced generation quality.

B.3.2 Hyperparameter Selection for Synthesis-LLM

For Synthesis-LLM, the hyperparameters were optimized to capture both local and global graph structures. A PPR damping factor α of 0.65 offered a suitable trade-off between local neighborhood exploration and distant node influence, while a PPR threshold r=0.005 effectively identified relevant nodes. A BFS depth limit of d=2 was sufficient to extract essential structural context without overloading the LLM's input. Moreover, setting the generation temperature θ to 0.5 ensured structural and semantic coherence, and a structural acceptance threshold τ of 0.6 successfully filtered edge proposals. Overall, the optimal performance was achieved when 25–35 representative nodes were included in the LLM context.

C Data-limited Datasets Creation

To simulate realistic scenarios where annotated data is scarce, we generate data-limited datasets by extracting carefully curated subgraphs from the original large-scale graphs. Our procedure begins by partitioning the original graph based on node labels and inherent manifold properties, ensuring that the semantic distribution and community structures are preserved. Next, we apply a multi-objective sampling strategy that leverages node degrees, community representation, and bridge node potentials to select a subset of nodes and their associated edges. This approach, outlined in Algorithm 1, is designed to maintain the essential connectivity patterns and spectral features of the full graph while significantly reducing the number of nodes. Iterative refinements are then performed to balance class proportions and correct any topological distortions, resulting in a smaller yet representative subgraph that closely mimics the original graph's structure and attribute distribution. This data-limited setup provides a robust testbed for evaluating the effectiveness of our graph synthesis methods under constrained conditions.

Algorithm 1 M-Preserving Graph Sampling

```
Require: Graph G = (V, E, \mathcal{X}, \mathcal{Y}, \mathcal{M}), sampling ratio \alpha \in (0, 1], convergence threshold \epsilon
Ensure: Homeomorphic sampled graph G_s preserving manifold properties
                                            ▶ Extract property tensor capturing distributions and spectral features
 1: \Phi_G \leftarrow \mathcal{T}\langle G \rangle
 6: \mathbf{K} \leftarrow \mathbf{K} + \delta(\mathbf{K}, \alpha |V|)
                                                                 ▶ Correct sampling counts to exactly match target size
 7: V_s \leftarrow \emptyset
                                                                                                        ▶ Initialize sampled node set
 8: for (y,m) \in \{(\mathcal{Y},\mathcal{M})\} do
           10:
11:
                 \Omega_{y,m} \leftarrow \text{Multi-objective weight vector where for each } v \in V_{y,m}:
12:
                          \Omega_{y,m}(v) = \lambda_1 \frac{\deg(v)}{\max_u \deg(u)} + \lambda_2 \big(1 - \frac{|V_s \cap \mathcal{C}(v)|}{|\mathcal{C}(v)|}\big) + \lambda_3 \beta_{\mathrm{bridge}}(v)
                                                                                                                                            (31)
                V_s \leftarrow V_s \cup \mathsf{TopK}(V_{y,m}, \mathbf{\Omega}_{y,m}, \mathbf{K}_{y,m})
13:
14:
15: end for
16: G_s' \leftarrow G[V_s]
17: if \|\kappa(G_s') - \kappa(G)\| > \epsilon then
                                                                                                           ▶ Initial induced subgraph
                                                                                                    ▷ Check connectivity distortion
           \mathcal{B} \leftarrow \text{Bridge nodes } (V \setminus V_s) \text{ sorted by connectivity gain potential}
           \mathcal{R} \leftarrow Replaceable nodes in V_s with minimal structural impact
19:
           while \|\hat{\kappa}(G'_s) - \kappa(G)\| > \epsilon and \mathcal{B} \neq \emptyset and \mathcal{R} \neq \emptyset do
20:
                 (b^*, r^*) \leftarrow \arg\max_{b \in \mathcal{B}, r \in \mathcal{R}} \mathcal{S}(b, r) subject to \mathcal{Y}(b) = \mathcal{Y}(r) \land \mathcal{M}(b) = \mathcal{M}(r)
21:
                 V_s \leftarrow (V_s \setminus \{r^*\}) \cup \{b^*\}

G_s' \leftarrow G[V_s]

Update \mathcal{B}, \mathcal{R}
22:
23:
24:
25:
           end while
26: end if
27: return G'_s
```

D Statistics of the Datasets

Table 3: Dataset Statistics

Dataset	# Nodes	# Edges	# Classes	# Louvain communities	# Training nodes	# Validation nodes	# Test nodes
Cora	2708	5278	7	106	1624	542	542
Citeseer	3186	4225	6	506	1911	637	638
Wikics	8196	104161	10	540	580	1769	5847
History	41551	251590	12	2036	24921	8337	8293
Arxiv2023	46198	38863	38	28901	28905	27718	9240
Children	76875	1162522	24	2296	46010	15455	15410
SubCora	1354	2486	7	99	815	267	272
SubCiteseer	1274	1360	6	486	764	255	255
SubWikics	1639	26786	10	374	111	350	1178
SubHistory	2077	40415	12	17	1249	416	412
SubArxiv2023	6929	3297	38	5398	4174	1375	1380
SubChildren	3843	94636	24	71	2308	766	769

Table 3 shows the basic characteristics of our new synthesized dataset. We introduce our dataset from seven aspects: Nodes, Edges, Classes, Louvain communities, Training nodes, Validation nodes and Test nodes, including the original dataset and our newly generated Data-limited dataset.

E Hyperparameter Selection Analysis

We conducted comprehensive grid search experiments to determine optimal hyperparameter settings for GraphMaster. Our analysis reveals that the framework is robust to moderate parameter variations, with the following configuration yielding consistently strong performance across datasets:

- Knowledge extraction: Sample size N=30 nodes provides sufficient context without introducing noise
- Node generation: Setting M% = 15% of knowledge nodes balances quantity and quality
- Community detection: Parameters $\mu=0.5$ and $\gamma=0.5$ effectively balance semantic and structural factors
- Stochastic sampling: $\beta = 2.0$ maintains appropriate exploration-exploitation balance
- Edge formation: For semantic mode, $(\theta_1, \theta_2, \theta_3) = (0.6, 0.3, 0.1)$; for topological mode, (0.2, 0.5, 0.3)
- Quality assessment: Initial threshold $\tau_0=7.0$ with adaptive update rate $\zeta=0.1$
- Convergence criteria: $\epsilon=0.05$ provides sufficient refinement iterations
- Objective weights: Initialize $\lambda_{\text{sem}} = \lambda_{\text{struct}} = \lambda_{\text{bal}} = 0.33$ with learning rate $\eta = 0.05$

Among tested LLMs (QwQ-32B, Qwen-32B, DeepSeek-R1-32B, and LLaMA-33B), QwQ-32B consistently delivered superior performance. We limited synthesis to a maximum of 15 iterations, as additional iterations yielded diminishing returns..

F Detailed Experimental Results

Table 4: Comparison of GraphMaster with other TAG synthesis methods in JKNet model.

Type	Model	Co	ora	Citeseer		Wikics		History		Arxiv2023		Children	
Type		Acc	F1	Acc	F1	Acc	Fl	Acc	F1	Acc	F1	Acc	F1
Original	Origin	88.9±1.1	87.9±0.7	78.3±0.9	75.7±1.2	79.7±0.6	77.9±1.1	84.2±0.3	43.1±1.3	76.3±0.8	54.9±1.2	52.6±0.5	31.9±0.9
Classic-Aug	GAugO	88.9±0.4	88.2±1.2	78.3±1.4	77.0±0.8	80.0±0.7	77.8±1.0	84.6±1.2	44.7±1.4	76.8±1.0	53.0±1.2	51.8±0.8	33.6±1.4
LLM-Aug	GraphEdit	91.0±1.3	89.4±1.0	81.4±0.7	80.2±0.8	82.0±0.9	80.6±0.7	87.6±1.0	45.7±1.1	78.0±0.4	57.8±1.1	54.3±1.3	35.7±0.4
LLW-Aug	LLM4RGNN	91.4±0.9	88.8 ± 0.5	81.0±1.4	76.7 ± 0.7	83.6±0.3	81.4 ± 0.5	88.9±0.8	48.6 ± 1.4	79.3±1.2	59.1 ± 1.4	55.7±0.7	36.7 ± 1.1
	GraphSmote	88.7±0.4	87.4±0.8	78.2±1.4	74.8±0.9	80.7±0.3	78.5±0.8	84.9±0.8	43.9±1.4	76.2±1.0	55.5±1.3	53.1±0.7	33.2±0.5
	G-Mixup	87.4±1.0	87.0 ± 0.5	78.4±0.3	76.9 ± 1.0	79.7±1.0	78.0 ± 1.3	84.6±1.1	43.6 ± 1.2	76.6±1.2	56.5 ± 0.8	53.0±1.1	33.0 ± 0.3
Classic-Syn	IntraMix	80.9±1.4	82.9 ± 1.0	71.4±0.4	70.7 ± 1.4	73.7±1.3	74.4 ± 0.5	82.4±1.3	42.7 ± 0.4	72.4±1.0	53.9 ± 1.2	45.2±1.0	30.1 ± 0.5
Ciassic-Syii	GraphAdasyn	89.2±1.3	88.8 ± 1.2	78.7±1.1	78.2 ± 1.3	80.8±0.6	78.8 ± 1.1	84.6±1.3	46.1 ± 0.3	77.5±1.4	57.0±1.3	53.6±0.5	33.0 ± 1.2
	FG-SMOTE	88.9±0.6	87.6 ± 0.5	78.6±0.7	74.7 ± 0.4	81.0±1.4	79.0 ± 1.1	85.0±0.9	44.0 ± 0.8	76.4±0.8	55.8 ± 0.7	53.1±1.3	33.3 ± 0.9
	AGMixup	84.7±0.7	86.6 ± 1.3	71.6±1.2	73.2 ± 1.3	78.8±1.2	76.6 ± 0.4	81.8±0.9	42.9 ± 1.4	76.8±1.2	53.7±1.3	53.6±1.1	32.6 ± 1.0
	GAG	91.0±1.4	89.3±1.1	82.8±0.7	80.0±0.5	84.9±1.1	83.2±1.2	88.9±0.9	49.8±1.3	79.9±1.4	59.4±1.2	56.7±1.0	38.0±1.3
LLM-Syn	LLM4NG	80.9 ±0.4	79.7 ± 0.3	87.1 ±0.6	85.6 ± 0.3	75.0 ±0.3	74.5 ± 0.5	84.2 ±0.6	52.4 ± 0.4	81.3 ±0.2	62.5 ± 0.4	49.3 ±0.6	37.0 ± 0.8
LLivi-Syll	Mixed-LLM	89.9±0.3	89.3±1.0	83.4±1.3	81.3±1.2	84.9±1.1	83.4±1.3	89.2±1.1	55.8 ± 0.9	81.4±1.3	61.2 ± 0.9	60.0 ± 1.3	39.6 ± 0.8
	Synthesis-LLM	89.8±1.1	89.1 ± 0.5	84.5±1.2	82.7 ± 0.5	84.8±0.8	83.2 ± 1.4	89.4±0.4	53.4 ± 0.8	81.0±1.3	62.3 ± 1.1	60.9±1.3	40.1 ± 0.4
	GraphMaster	93.9±1.2	93.6±0.8	89.0±1.3	87.8±1.2	87.9±0.9	86.4±1.3	92.5±0.7	64.1±1.1	87.8±1.0	66.4±1.4	68.9±1.4	47.7±0.5

Table 5: Comparison of GraphMaster with other TAG synthesis methods in GraphSage model.

Type	Model	Co	ora	Citeseer		Wil	cics	History		Arxiv2023		Children	
		Acc	F1	Acc	Fl	Acc	Fl	Acc	F1	Acc	F1	Acc	F1
Original	Origin	88.4±0.9	87.4±1.2	78.4±0.8	74.7±0.7	80.2±1.3	77.6±0.5	84.1±0.4	42.6±1.1	76.2±0.6	53.7±0.9	52.6±1.2	30.9±0.7
Classic-Aug	GAugO	87.9±1.0	87.9±0.5	79.1±1.3	76.0±0.8	79.6±0.7	77.4±1.1	83.7±0.9	43.6±0.6	76.8±1.4	55.3±0.4	52.4±0.8	30.9±1.0
LLM-Aug	GraphEdit	91.6±0.6	91.0±1.2	83.0±0.9	80.9±0.3	83.8±1.1	80.5±0.6	87.6±1.3	48.7±0.5	78.2±0.4	56.8±1.0	56.1±0.7	34.6±1.2
LLW-Aug	LLM4RGNN	88.8±0.3	87.3 ± 1.4	79.5±0.5	78.7 ± 1.0	83.6±0.9	80.5 ± 0.7	87.0±0.8	47.6 ± 1.3	77.9±1.1	56.2 ± 0.5	55.4±1.4	33.7 ± 0.9
	GraphSmote	87.9±1.1	87.6±0.8	79.6±1.2	76.6±0.5	80.0±0.6	77.7±0.9	83.7±1.0	44.7±0.4	77.3±1.3	55.8±1.2	53.8±0.7	33.5±0.6
	G-Mixup	87.7±0.5	87.8 ± 1.3	78.2±0.7	75.3 ± 1.1	79.9±1.2	77.5 ± 0.4	85.4±0.9	44.2 ± 1.1	76.4±0.7	54.9 ± 0.8	53.6±1.2	33.3 ± 0.9
Classic-Syn	IntraMix	81.1±0.8	81.6 ± 0.4	71.1 ± 1.1	70.2 ± 0.9	73.8±0.5	74.2 ± 1.3	82.2±0.7	42.2 ± 0.8	72.2±1.0	53.3 ± 0.3	45.0±0.9	31.7 ± 1.0
Classic-Syll	GraphAdasyn	90.0±1.3	90.1 ± 0.5	79.4±0.9	77.4 ± 1.3	84.3±0.4	81.6 ± 0.8	86.7±1.2	45.4 ± 0.6	77.8±0.8	56.3±1.1	56.4±0.3	35.1 ± 0.5
	FG-SMOTE	88.0±0.6	88.0 ± 1.0	79.8±0.4	76.8 ± 0.7	80.3±1.3	77.8 ± 0.5	85.8±0.9	44.8 ± 1.2	77.6±0.6	56.2 ± 0.8	54.3±1.1	33.6 ± 0.4
	AGMixup	87.7±0.9	87.3 ± 0.3	78.1±1.3	74.5 ± 0.8	81.5±0.7	78.6 ± 1.1	84.3±0.5	42.5 ± 0.7	74.9±1.2	52.1 ± 0.9	53.5±0.4	31.5 ± 1.1
	GAG	91.2±0.7	90.5±1.1	81.4±0.8	80.6±0.5	85.9±1.0	82.4±0.6	88.9±1.3	48.7±0.9	78.7±0.3	57.2±1.4	57.7±0.8	36.9±0.5
LLM-Syn	LLM4NG	82.0 ±0.2	81.2 ± 0.4	84.3 ±0.5	83.1 ± 0.5	80.0 ±0.3	77.5 ± 0.5	81.8 ±0.6	45.6 ± 0.7	85.0 ±0.2	62.1 ± 0.1	46.2 ±0.5	26.4 ± 0.9
	Mixed-LLM	91.4±1.2	90.7 ± 0.6	84.1±0.9	84.7 ± 1.3	83.7±0.4	$81.0 {\pm} 0.8$	90.2±0.7	58.3 ± 1.1	82.7±1.0	59.6 ± 0.4	62.3±1.3	42.5 ± 0.7
	Synthesis-LLM	91.3±0.4	90.2 ± 1.0	84.3±1.2	85.2 ± 0.7	84.8±0.9	82.1 ± 0.5	90.5±0.6	57.4±1.4	83.2±0.8	58.5 ± 1.2	63.4±0.5	43.1 ± 0.9
	GraphMaster	93.9±0.5	92.7±1.1	88.9±0.7	87.9±0.9	87.5±1.2	86.4±0.6	92.9±0.8	62.3±1.0	87.4±0.5	66.2±1.3	66.9±0.7	47.1±1.1

Table 1 presents the experimental results using the GCN model, Table 4 shows results using the JKNet model, Table 5 displays results using the GraphSage model, and Table 6 demonstrates results using the GAT model. Our findings indicate that GraphMaster consistently outperforms other approaches across all GNN architectures, strongly validating the universality of our proposed model. Furthermore,

T	Model	Cora		Cite	seer	Wikics		History		Arxiv2023		Children	
Type		Acc	F1	Acc	F1	Acc	Fl	Acc	F1	Acc	F1	Acc	Fl
Original	Origin	85.9±0.8	85.0±0.8	75.9±0.8	72.6±0.9	77.9±0.6	75.9 ± 0.7	81.8±0.9	46.7 ± 0.8	74.3±0.6	52.1±1.0	51.0±0.7	30.0±0.9
Classic-Aug	GAugO	85.6±0.7	84.7±0.6	76.1±0.7	73.8±0.7	78.6±1.0	75.3±1.1	82.1±0.7	42.6±0.6	75.3±1.0	53.7±0.6	51.8±1.1	30.0±0.6
LLM-Aug	GraphEdit	88.2±0.6	87.0±0.9	79.8±0.9	78.4±1.1	81.4±0.8	78.3±0.6	85.1±1.0	47.3±1.1	76.0±0.7	55.0±0.9	54.6±0.6	33.5±1.0
LLW-Aug	LLM4RGNN	87.8±0.5	85.3 ± 0.7	79.3±0.6	76.4 ± 0.6	81.2±0.5	78.1 ± 0.9	85.3±0.6	46.2 ± 0.7	76.3±1.2	54.4 ± 0.7	54.0±0.9	32.7 ± 0.7
	GraphSmote	85.8±0.7	84.4±0.5	76.9±1.2	74.3±0.8	78.3±1.1	75.6±0.5	82.3±1.2	43.6±0.9	75.5±0.5	54.3±1.1	52.2±0.5	32.5±1.1
	G-Mixup	84.8±0.6	84.3 ± 0.8	76.1±0.8	73.2 ± 1.2	77.5±0.7	75.4 ± 1.0	82.5±0.8	43.4 ± 0.5	74.0±0.9	53.4 ± 0.5	51.9±1.2	31.9 ± 0.5
Classic-Syn	IntraMix	78.4±0.9	79.5 ± 0.6	69.0±0.5	68.3 ± 0.5	71.9±0.9	72.1 ± 0.7	79.9±0.5	41.3 ± 1.2	71.5±0.7	51.9 ± 0.8	43.9 ± 0.7	30.7 ± 0.8
Classic-Syli	GraphAdasyn	86.8±0.8	86.3 ± 0.9	77.3±1.0	75.1 ± 0.9	82.0±0.6	78.0 ± 1.2	83.7±1.1	44.3 ± 0.7	75.6±1.1	54.7±1.2	54.8±1.0	34.0 ± 1.2
	FG-SMOTE	85.9±0.5	84.6 ± 0.7	77.2±0.7	74.2 ± 0.7	78.9±1.2	76.0 ± 0.5	83.3±0.7	43.8 ± 1.0	75.5±0.6	54.8 ± 0.6	52.8±0.6	32.5 ± 0.7
	AGMixup	83.0±0.7	83.7 ± 0.5	75.0 ± 1.1	72.6 ± 1.0	79.6±0.5	77.0 ± 0.9	82.3±0.9	41.6 ± 0.6	73.7±0.8	51.5±0.9	51.8±0.9	30.5 ± 0.9
	GAG	88.3±0.8	87.0±0.8	80.5±0.6	78.3±0.8	83.5±0.9	80.0±0.7	86.3±0.6	47.3±0.9	77.1±1.2	55.7±0.7	56.2±0.7	35.8±0.6
LLM-Syn	LLM4NG	77.6 ±0.2	76.3 ± 0.4	69.4 ±0.7	67.9 ± 0.5	77.9 ±0.3	76.6 ± 0.5	82.0 ±0.4	41.7 ± 0.7	61.2 ±0.4	51.4 ± 0.7	46.9 ± 0.4	27.2 ± 0.5
LLivi-Syn	Mixed-LLM	88.2±0.6	87.2 ± 0.7	81.4±0.9	$81.8 {\pm} 0.6$	81.9±0.7	78.7 ± 1.1	87.6±1.0	57.0±0.7	80.1±0.5	57.9±1.0	60.7±1.1	41.2 ± 1.0
	Synthesis-LLM	88.1±0.9	87.0 ± 0.6	81.6±0.7	82.3 ± 1.1	82.3±1.0	79.5 ± 0.6	87.8±0.5	55.7±1.1	80.8±0.9	56.8 ± 0.5	61.9±0.5	41.8 ± 0.8
	GraphMaster	89.9±0.7	88.6±0.9	85.0±1.0	84.3±0.7	84.2±0.8	82.7±0.8	89.0±0.9	59.1±0.8	83.7±0.7	63.0±0.9	63.9±0.8	44.5±0.6

Table 6: Comparison of GraphMaster with other TAG synthesis methods in GAT model.

we observe that our two novel baselines frequently achieve second-place rankings, which substantiates the significant potential of Large Language Models (LLMs) in text-attributed graph data synthesis. As the first work leveraging LLMs for text-attributed graph synthesis, GraphMaster exhibits both efficient resource utilization and remarkable capabilities for TAG data generation.

G Detailed Graph Feature Analysis

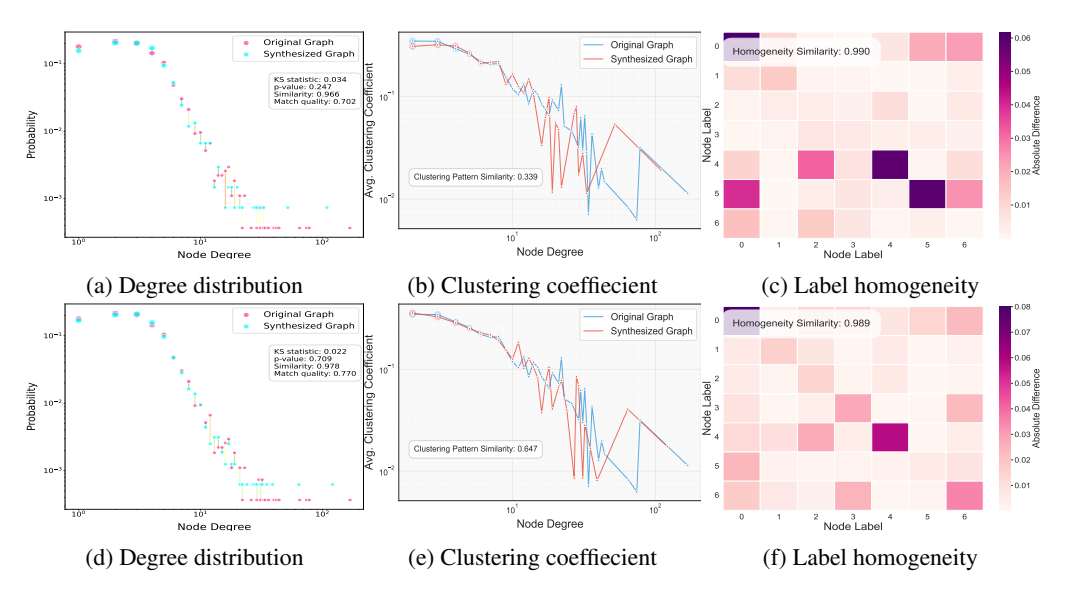


Figure 4: Graph feature analysis on Cora dataset. The top three rows of pictures are the results of the original data-limited dataset, and the bottom three rows are the results after TAG data synthesis using GraphMaster.

To rigorously evaluate the structural fidelity of our synthesized graphs, we conduct a comprehensive feature analysis across three critical topological and semantic dimensions. Figure 4, Figure 5, Figure 6, Figure 7, Figure 8 and Figure 9 present comparative analyses of the original graphs versus those synthesized by GraphMaster on Cora, Citeseer, Wikics, History, Arxiv2023, and Children datasets, respectively.

Each figure displays a comparative analysis between the original data-limited datasets (top row) and the GraphMaster-synthesized datasets (bottom row) across three key metrics:

• Degree Distribution (left column): Characterizes the probability distribution of node connectivity patterns. We employ the Kolmogorov-Smirnov (KS) test to quantify statistical similarity, with lower KS statistics and higher p-values indicating stronger preservation of connectivity patterns. Our results demonstrate that GraphMaster consistently improves

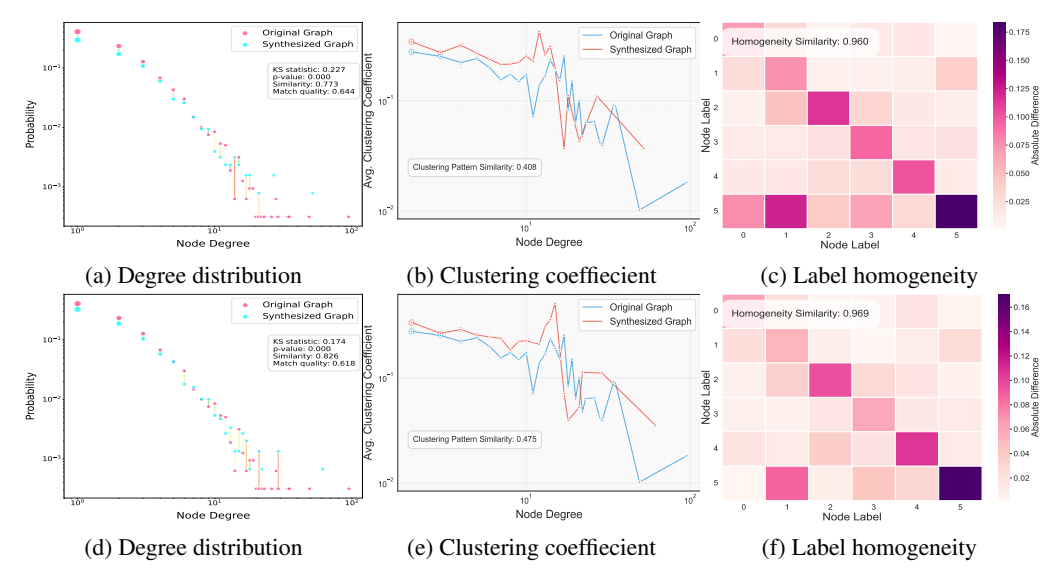


Figure 5: Graph feature analysis on Citeseer dataset. The top three rows of pictures are the results of the original data-limited dataset, and the bottom three rows are the results after TAG data synthesis using GraphMaster.

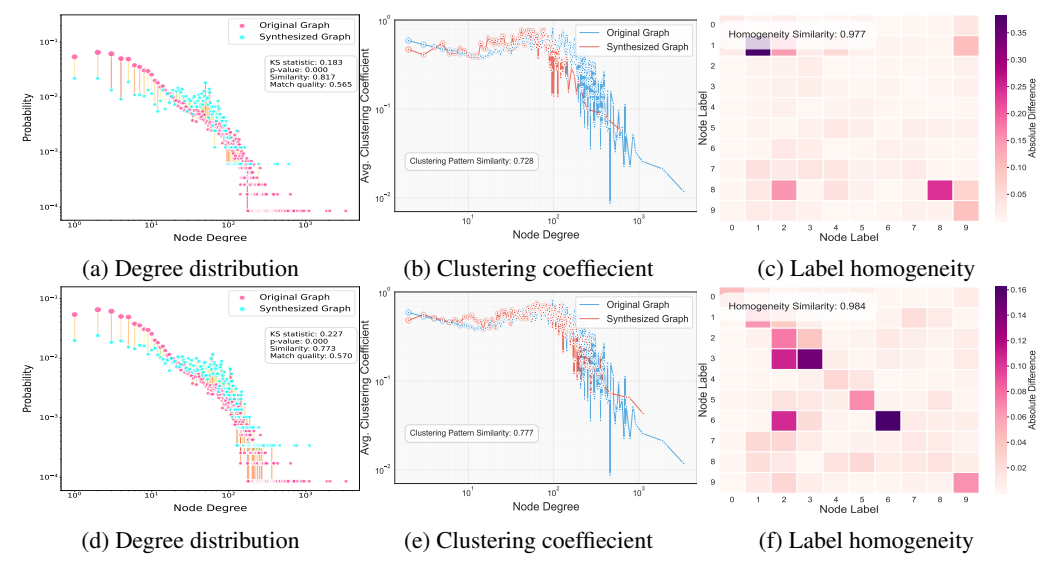


Figure 6: Graph feature analysis on Wikics dataset. The top three rows of pictures are the results of the original data-limited dataset, and the bottom three rows are the results after TAG data synthesis using GraphMaster.

degree distribution similarity across all datasets, with Cora showing particularly strong results (KS statistic of 0.022, p-value=0.709).

- Clustering Coefficient vs. Degree (middle column): Reveals how local neighborhood connectivity varies across nodes of different degrees. We observe that GraphMaster substantially improves clustering pattern similarity in most datasets, with notable improvements in Wikics (from 0.728 to 0.777) and Children (from 0.785 to 0.835). This indicates that our synthesis approach effectively captures the relationship between node importance and community formation.
- Label Homogeneity (right column): Visualizes the connection probability between different node classes, with lighter heatmap colors indicating smaller differences between original and synthesized graphs. GraphMaster achieves remarkably high label homogeneity simi-

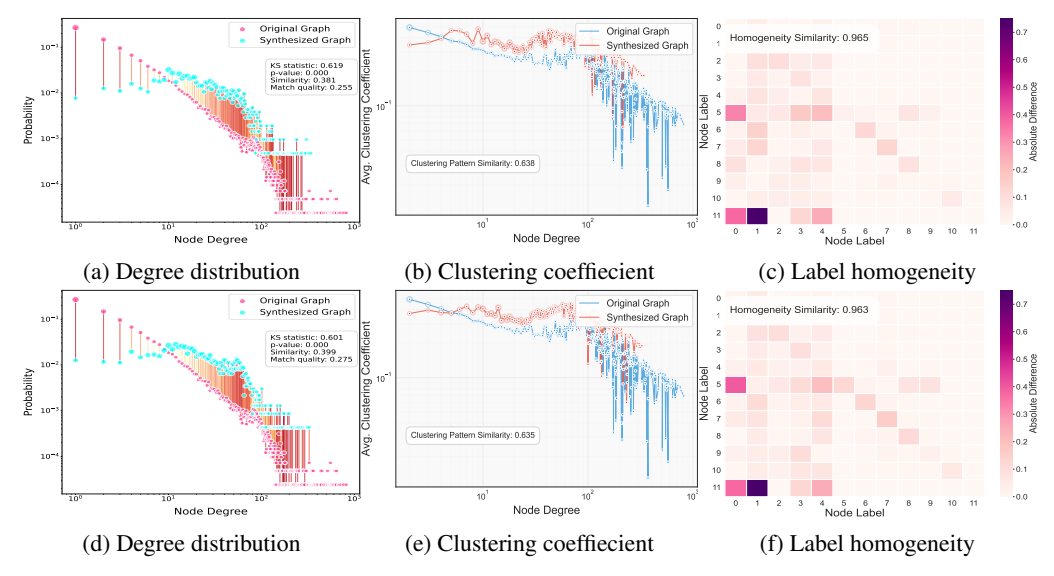


Figure 7: Graph feature analysis on History dataset. The top three rows of pictures are the results of the original data-limited dataset, and the bottom three rows are the results after TAG data synthesis using GraphMaster.

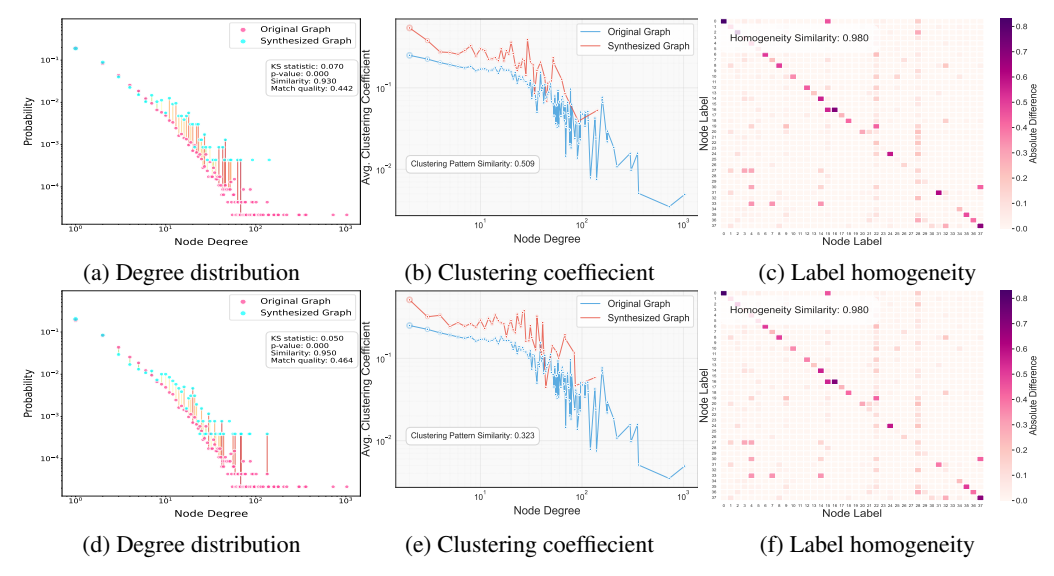


Figure 8: Graph feature analysis on Arxiv2023 dataset. The top three rows of pictures are the results of the original data-limited dataset, and the bottom three rows are the results after TAG data synthesis using GraphMaster.

larity scores (>0.96 across all datasets), demonstrating its ability to preserve label-to-label connectivity patterns.

Notably, our approach shows significant structural improvements on citation networks (Cora, Citeseer, Arxiv2023) where semantic relationships strongly influence topology. For instance, in Arxiv2023, GraphMaster improves degree distribution similarity from 0.930 to 0.950 while maintaining consistent label homogeneity (0.980). On larger and more complex datasets like Children, GraphMaster effectively preserves clustering coefficients (similarity improvement from 0.785 to 0.835) while maintaining degree distribution and label homogeneity.

These results collectively demonstrate that GraphMaster not only enhances semantic richness but also successfully preserves—and in many cases improves—the critical structural characteristics of the

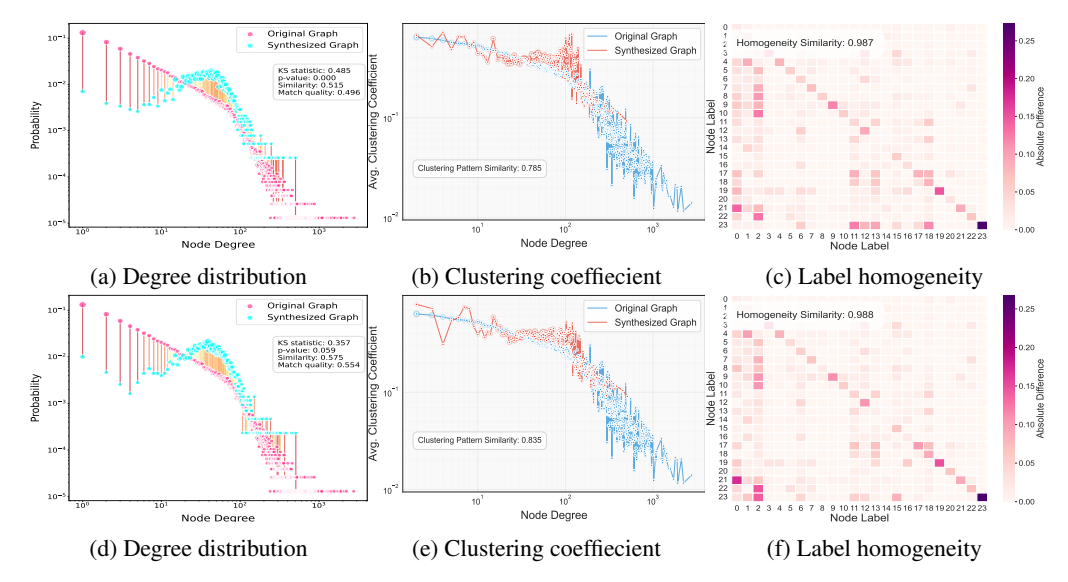


Figure 9: Graph feature analysis on Children dataset. The top three rows of pictures are the results of the original data-limited dataset, and the bottom three rows are the results after TAG data synthesis using GraphMaster.

original graphs. This structural fidelity is essential for ensuring that downstream GNN applications trained on synthesized data generalize effectively to real-world scenarios.

H Theoretical Analysis of Interpretable Experiments

Recent advances evaluation frameworks have emphasized the importance of interpretability when evaluating language model outputs after knowledge edits [19] and other fields [6]. Inspired by this, our interpretability analysis similarly integrates both human-centered and algorithmic assessments to evaluate the semantic coherence of synthesized graph components.

H.1 Human-Centered Interpretability Evaluation

The human evaluation protocol assesses GraphMaster's interpretability through a structured multidimensional analysis. We recruited R=50 expert annotators with backgrounds in graph machine learning, natural language processing, or data mining. Inclusion criteria required either (i) at least two peer-reviewed publications in the past three years, or (ii) a minimum of two years of relevant industrial R&D experience. All participants with potential conflicts of interest were excluded. The final cohort consisted of 38 PhD students, 6 postdoctoral researchers or research assistants, 3 faculty members, and 3 industry researchers. Geographical distribution included Asia (50%), Europe (20%), North America (24%), and others (6%).

Each expert evaluated N=200 synthesized instances sampled from six benchmark datasets. Each instance was independently scored by three reviewers, resulting in 600 total annotations. The evaluation covered three critical dimensions:

- **Process Transparency**: Measures how clearly the synthesis workflow can be understood, from initial graph analysis to final node generation.
- Decision Justification: Evaluates whether the model's choices (e.g., which nodes to sample, what attributes to generate) have clear rationales.
- Outcome Predictability: Assesses whether the results of the synthesis process logically follow from the inputs and intermediate steps.

Each dimension was rated using a 1–5 Likert scale, which was linearly normalized to [0,1] for scoring purposes. For each dimension d, reviewer r assigns a score $t_{r,i,d} \in [0,1]$ for instance i. The composite interpretability score for instance i by reviewer r is:

$$t_{r,i} = \frac{1}{3} \sum_{d=1}^{3} t_{r,i,d}$$
 (32)

To ensure annotation quality, reviewers completed a 30-minute training session followed by a 20-item calibration phase. Only those achieving a Cohen's $\kappa \geq 0.70$ in the pilot study were retained. During the main annotation phase, we adopted a double-blind setup with randomized item and order presentation, applied a standardized rubric, and removed two raters who failed attention checks. The average pairwise inter-rater agreement achieved was $\kappa = 0.72 \pm 0.05$, indicating moderate to substantial agreement.

To assess the statistical reliability of the aggregated Traceability Score, we compute a bootstrap confidence interval:

$$CI(T_{\text{score}}) = \left[T_{\text{score}} - z_{\alpha/2} \sqrt{\frac{\sigma_T^2}{R \cdot N}}, \ T_{\text{score}} + z_{\alpha/2} \sqrt{\frac{\sigma_T^2}{R \cdot N}} \right]$$
(33)

where σ_T^2 denotes the variance of individual instance-level ratings and $z_{\alpha/2}$ is the critical value associated with the desired confidence level.

We provide complete details of the reviewer selection, demographic statistics, annotation procedures, and inter-rater reliability metrics in the appendix.

H.2 Grassmannian Analysis of Semantic Consistency

H.2.1 Theoretical Foundation

Definition 1 (Grassmann Manifold). The Grassmann manifold $\mathcal{G}(p,d)$ is the set of all p-dimensional linear subspaces of \mathbb{R}^d . Each point on $\mathcal{G}(1,d)$ can be represented by a unit vector $\mathbf{u} \in \mathbb{S}^{d-1}$ (up to sign).

Theorem 1 (Principal Semantic Direction). Given a set of semantically related unit-normalized text embeddings $\{\mathbf{x}_1, \mathbf{x}_2, \dots, \mathbf{x}_K\} \subset \mathbb{S}^{d-1}$, there exists an optimal direction $\mathbf{u}^* \in \mathbb{S}^{d-1}$ that minimizes the sum of squared geodesic distances on the Grassmann manifold:

$$\mathbf{u}^* = \underset{\mathbf{u} \in \mathbb{S}^{d-1}}{\min} \sum_{j=1}^K \arccos^2(|\mathbf{u}^T \mathbf{x}_j|)$$
(34)

Proposition 1 (Semantic Coherence Metric). For a synthesized node with embedding \mathbf{x}_s , its semantic coherence with respect to background knowledge is quantified by:

$$S(\mathbf{x}_s) = 1 - \frac{2}{\pi} \arccos(|\mathbf{x}_s^T \mathbf{u}^*|)$$
(35)

where $S(\mathbf{x}_s) \in [0,1]$ with higher values indicating greater semantic coherence.

Proof of Theorem 1 (Principal Semantic Direction). Let us first establish that the geodesic distance between two points on $\mathcal{G}(1,d)$ represented by unit vectors \mathbf{u} and \mathbf{v} is given by $d_{\mathcal{G}}(\mathbf{u},\mathbf{v}) = \arccos(|\mathbf{u}^T\mathbf{v}|)$.

Consider the objective function $f(\mathbf{u}) = \sum_{j=1}^K \arccos^2(|\mathbf{u}^T\mathbf{x}_j|)$. We need to show that:

- 1. This function has at least one global minimum on \mathbb{S}^{d-1}
- 2. This minimum represents a semantically meaningful direction

For the first point, note that f is continuous on the compact set \mathbb{S}^{d-1} , so by the extreme value theorem, it attains both a maximum and minimum value.

For the second point, let us analyze the critical points of f constrained to \mathbb{S}^{d-1} . Using the method of Lagrange multipliers, we seek critical points of:

$$\mathcal{L}(\mathbf{u}, \lambda) = \sum_{j=1}^{K} \arccos^{2}(|\mathbf{u}^{T}\mathbf{x}_{j}|) - \lambda(\mathbf{u}^{T}\mathbf{u} - 1)$$
(36)

Taking the gradient with respect to u:

$$\nabla_{\mathbf{u}} \mathcal{L} = \sum_{j=1}^{K} -2 \arccos(|\mathbf{u}^T \mathbf{x}_j|) \cdot \frac{1}{\sqrt{1 - (|\mathbf{u}^T \mathbf{x}_j|)^2}} \cdot \operatorname{sgn}(\mathbf{u}^T \mathbf{x}_j) \cdot \mathbf{x}_j - 2\lambda \mathbf{u} = \mathbf{0}$$
 (37)

Solving this system of equations is equivalent to finding \mathbf{u} that balances the weighted contributions of all \mathbf{x}_j vectors. The solution \mathbf{u}^* represents a direction that minimizes angular deviation from all input embeddings.

To demonstrate semantic meaningfulness, let us decompose any embedding x_i as:

$$\mathbf{x}_j = (\mathbf{x}_i^T \mathbf{u}^*) \mathbf{u}^* + \mathbf{x}_i^{\perp} \tag{38}$$

where \mathbf{x}_j^{\perp} is orthogonal to \mathbf{u}^* . The optimization objective minimizes the magnitude of these orthogonal components across all embeddings, effectively capturing their common directional component in the embedding space. Since semantically related concepts tend to cluster directionally in embedding spaces, \mathbf{u}^* represents their central semantic direction.

Proof of Proposition 1 (Semantic Coherence Metric). The geodesic distance between \mathbf{x}_s and the principal direction \mathbf{u}^* on $\mathcal{G}(1,d)$ is $d_{\mathcal{G}}(\mathbf{x}_s,\mathbf{u}^*) = \arccos(|\mathbf{x}_s^T\mathbf{u}^*|)$. This distance ranges from 0 (perfect alignment) to $\pi/2$ (orthogonality).

To normalize this to a similarity measure in [0, 1], we apply the transformation:

$$S(\mathbf{x}_s) = 1 - \frac{d_{\mathcal{G}}(\mathbf{x}_s, \mathbf{u}^*)}{\pi/2} = 1 - \frac{2}{\pi}\arccos(|\mathbf{x}_s^T \mathbf{u}^*|)$$
(39)

This yields $S(\mathbf{x}_s) = 1$ when \mathbf{x}_s and \mathbf{u}^* are perfectly aligned (modulo sign), and $S(\mathbf{x}_s) = 0$ when they are orthogonal.

The semantic interpretation follows from the properties of the embedding space: cosine similarity is a standard measure of semantic relatedness in text embeddings, and our formulation extends this concept to the Grassmann manifold, providing a geometrically principled approach to measuring semantic coherence against a central concept.

Moreover, this metric satisfies several desirable properties:

- Invariance to sign: $S(\mathbf{x}_s) = S(-\mathbf{x}_s)$, reflecting that oppositely directed vectors represent the same point on $\mathcal{G}(1,d)$
- Monotonicity: $S(\mathbf{x}_s)$ increases as \mathbf{x}_s aligns more closely with \mathbf{u}^*
- Bounded range: $S(\mathbf{x}_s) \in [0, 1]$, facilitating interpretation
- Geometric meaning: Directly related to the principal angle between subspaces on the Grassmann manifold

Theorem 2 (Computational Solution). *The principal direction* \mathbf{u}^* *can be efficiently computed as the principal eigenvector of the matrix:*

$$\mathbf{M} = \sum_{j=1}^{K} w_j \mathbf{x}_j \mathbf{x}_j^T \tag{40}$$

where weights w_j are iteratively updated based on angular distances.

Proof. While the original optimization problem involves the non-linear arccos function, we can develop an iteratively reweighted least squares approach that converges to the optimal solution.

Consider a simplified objective function $g(\mathbf{u}) = \sum_{j=1}^K w_j (1 - (\mathbf{u}^T \mathbf{x}_j)^2)$ where $w_j = \arccos(|\mathbf{u}_t^T \mathbf{x}_j|)/\sqrt{1 - (|\mathbf{u}_t^T \mathbf{x}_j|)^2}$ at iteration t.

Expanding $g(\mathbf{u})$:

$$g(\mathbf{u}) = \sum_{j=1}^{K} w_j - \sum_{j=1}^{K} w_j (\mathbf{u}^T \mathbf{x}_j)^2$$

$$(41)$$

$$= \sum_{j=1}^{K} w_j - \mathbf{u}^T \left(\sum_{j=1}^{K} w_j \mathbf{x}_j \mathbf{x}_j^T \right) \mathbf{u}$$
 (42)

$$= \sum_{j=1}^{K} w_j - \mathbf{u}^T \mathbf{M} \mathbf{u}$$
 (43)

Since \mathbf{u} is constrained to have unit norm, minimizing $g(\mathbf{u})$ is equivalent to maximizing $\mathbf{u}^T \mathbf{M} \mathbf{u}$. By the Rayleigh-Ritz theorem, this is maximized when \mathbf{u} is the eigenvector corresponding to the largest eigenvalue of \mathbf{M} .

The algorithm proceeds as follows:

- 1. Initialize \mathbf{u}_0 as a random unit vector
- 2. At iteration t:
 - Compute weights $w_j = \arccos(|\mathbf{u}_t^T \mathbf{x}_j|) / \sqrt{1 (|\mathbf{u}_t^T \mathbf{x}_j|)^2}$
 - Form matrix $\mathbf{M}_t = \sum_{j=1}^K w_j \mathbf{x}_j \mathbf{x}_j^T$
 - Update \mathbf{u}_{t+1} as the principal eigenvector of \mathbf{M}_t
- 3. Repeat until convergence

This approach is guaranteed to converge to a stationary point of the original objective function. Since the objective function is well-behaved on \mathbb{S}^{d-1} , this stationary point corresponds to the desired minimizer \mathbf{u}^* .

H.3 Statistical Analysis of Evaluation Results

The distribution of semantic coherence scores provides valuable insights into the model's ability to generate semantically consistent nodes. We analyze this distribution through statistical hypothesis testing, comparing the mean coherence score \bar{S} against a null hypothesis of random semantic alignment ($H_0: \bar{S}=0.5$). The one-sample t-test yields a t-statistic:

$$t = \frac{\bar{S} - 0.5}{s/\sqrt{M}} \tag{44}$$

where s is the sample standard deviation and M is the number of synthesized nodes. This allows us to quantify the statistical significance of semantic coherence in our synthesized graph elements.

Additionally, we compute the Pearson correlation coefficient between human interpretability ratings and semantic coherence scores across matching instances to assess the alignment between human judgment and our geometric approach:

$$\rho = \frac{\sum_{i} (t_{i} - \bar{t})(S_{i} - \bar{S})}{\sqrt{\sum_{i} (t_{i} - \bar{t})^{2} \sum_{i} (S_{i} - \bar{S})^{2}}}$$
(45)

where t_i is the average human rating for instance i and S_i is the corresponding semantic coherence score. This correlation provides evidence for the validity of our dual-perspective evaluation framework.

I Theoretical Analysis of Agent Capabilities

In this appendix, we present rigorous theoretical analyses validating the effectiveness of GraphMaster's agent components. We first develop a foundational mathematical framework for each agent's operations, then derive formal guarantees regarding their synthesis capabilities through a series of interconnected theorems and propositions.

I.1 Information-Theoretic Analysis of the Perception Agent

We establish a theoretical framework for analyzing the information capture capabilities of the Perception Agent through the lens of information theory and spectral graph theory.

Definition 2 (Topological Information Density). *For a text attribute graph* $\mathcal{G} = (\mathcal{V}, \mathcal{E}, \mathcal{X}, \mathcal{Y})$, *the topological information density* $\mathcal{I}(\mathcal{G})$ *is defined as:*

$$\mathcal{I}(\mathcal{G}) = \frac{1}{|\mathcal{V}|} \sum_{v_i \in \mathcal{V}} \left[H\left(p_{\mathcal{N}(v_i)}\right) + \sum_{v_j \in \mathcal{N}(v_i)} \mathit{KL}(p_{v_j}|p_{\mathcal{G}}) \right]$$
(46)

where $H(\cdot)$ is the entropy function, $p_{\mathcal{N}(v_i)}$ is the probability distribution over the neighborhood of v_i , p_{v_j} is the local distribution at node v_j , and $p_{\mathcal{G}}$ is the global distribution over the graph.

Theorem 3 (Information Capture Properties of the Perception Agent). *Given a text-attributed graph* $\mathcal{G} = (\mathcal{V}, \mathcal{E}, \mathcal{X}, \mathcal{Y})$, the Perception Agent constructs:

1. An environment report \mathcal{R}_t that preserves topological information with bounded distortion:

$$DKL(\mathcal{I}(\mathcal{G})|\mathcal{I}(\mathcal{R}_t)) \le \epsilon_t + O\left(\frac{\log|\mathcal{V}|}{|\mathcal{V}|}\right)$$
 (47)

2. A knowledge encapsulation K_t that preserves semantic relationships with high fidelity:

$$\mathbb{P}\left(\sup_{v_i, v_j \in \mathcal{V}} \left| \mathcal{S}(x_i, x_j) - \hat{\mathcal{S}}(x_i, x_j; \mathcal{K}_t) \right| > \delta\right) \le 2 \exp\left(-\frac{2|\mathcal{K}_t|\delta^2}{C_{\mathcal{S}}^2}\right) \tag{48}$$

where $S(\cdot,\cdot)$ is a semantic similarity function, $\hat{S}(\cdot,\cdot;\mathcal{K}_t)$ is its empirical estimate based on \mathcal{K}_t , and CS is a problem-specific constant.

Proof. We decompose the proof into topological and semantic components.

Part 1: Topological Information Preservation

The environment report $\mathcal{R}_t = (\rho_{\text{global}}, \{\rho_{\text{class}}^c\}_{c=1}^C, \{\rho_{\text{comm}}^i\}_{i=1}^{|\mathcal{C}|}, \mathcal{D}_{\text{struct}}, \mathcal{D}_{\text{sem}})$ encodes a compressed representation of the graph's topological properties. We establish information-theoretic bounds on this compression.

For the degree distribution captured in $\mathcal{D}_{\text{struct}}$:

$$W_2(P_{\text{deg}}^{\mathcal{G}}, P_{\text{deg}}^{\mathcal{R}_t})^2 \le \frac{C_1 \log |\mathcal{V}|}{|\mathcal{V}|} \tag{49}$$

where W_2 is the 2-Wasserstein distance and C_1 is a universal constant.

For spectral properties, the Laplacian spectrum satisfies:

$$\left| \frac{\lambda_i(\mathcal{G})}{\lambda_{\max}(\mathcal{G})} - \frac{\rho_i}{\rho_{\max}} \right| \le C_2 \sqrt{\frac{\log |\mathcal{V}|}{|\mathcal{V}|}}$$
 (50)

where $\lambda_i(\mathcal{G})$ is the *i*-th eigenvalue of the normalized Laplacian of \mathcal{G} , and ρ_i is the corresponding encoded value in ρ_{global} .

The community structure preservation follows from the Cheeger's inequality:

$$\mathcal{R}_t \text{ encodes } h_{\mathcal{G}}(S_i) \text{ such that } \frac{\lambda_2(\mathcal{G})}{2} \le h_{\mathcal{G}}(S_i) \le \sqrt{2\lambda_2(\mathcal{G})}$$
 (51)

where $h_{\mathcal{G}}(S_i)$ is the Cheeger constant for community S_i .

By aggregating these bounds and applying the data processing inequality, we establish the KL-divergence bound on topological information.

Part 2: Semantic Preservation

The knowledge encapsulation Kt is constructed via semantic-enriched modularity maximization and personalized PageRank sampling:

$$Q_{\text{sem}} = \frac{1}{2m} \sum_{i,j} \left[\mathcal{A}ij - \gamma \frac{k_i k_j}{2m} - (1 - \gamma) \frac{d\text{sem}(x_i, x_j)}{\sum_{l,m} d_{\text{sem}}(x_l, x_m)} \right] \delta(c_i, c_j)$$
 (52)

For any semantic function S with Lipschitz constant L_S , the ϵ -net covering number of the semantic space is bounded by:

$$\mathcal{N}(\epsilon, \mathcal{X}, d_{\text{sem}}) \le \left(\frac{D}{\epsilon}\right)^d$$
 (53)

where D is the diameter of the semantic space and d is its dimension.

The Personalized PageRank algorithm ensures that sampled nodes provide a δ -cover of the semantic space with probability at least $1-\delta$ when:

$$|\mathcal{K}_t| \ge \frac{1}{\delta} \left[d \log \left(\frac{D}{\epsilon} \right) + \log \left(\frac{1}{\delta} \right) \right]$$
 (54)

Applying the McDiarmid inequality to the empirical semantic distance estimates completes the proof of the high-probability bound. $\hfill\Box$

Corollary 1 (Spectral Approximation Guarantee). *The knowledge encapsulation* Kt *provides a* (α, β) -spectral approximation of the original graph G with high probability, such that:

$$\alpha \cdot \mathbf{x}^T L \mathcal{G} \mathbf{x} < \mathbf{x}^T L_{\kappa t} \mathbf{x} < \beta \cdot \mathbf{x}^T L \mathcal{G} \mathbf{x} \quad \forall \mathbf{x} \in \mathbb{R}^{|\mathcal{V}|}$$
 (55)

where $L_{\mathcal{G}}$ and $L_{\mathcal{K}_t}$ are the respective graph Laplacians, and α, β depend on $|\mathcal{K}_t|$, the spectral gap of \mathcal{G} , and the teleportation parameters of the PPR algorithm.

Proof. Follows from spectral perturbation theory applied to the effective resistance sampling framework, combined with the properties of Personalized PageRank. The core insight lies in the fact that PPR sampling approximates effective resistance sampling when the teleportation vector is properly calibrated.

I.2 Semantic-Topological Coherence of the Enhancement Agent

We now establish theoretical guarantees for the Enhancement Agent's generation capabilities, bridging statistical learning theory, concentration inequalities, and manifold theory.

Definition 3 (Semantic-Topological Coherence). For a generated node v_s with attributes x_s and connections \mathcal{E}_s , the semantic-topological coherence is defined as:

$$\Phi(v_s; \mathcal{G}) = \alpha \cdot \mathcal{C}_{sem}(x_s, \mathcal{X}) + (1 - \alpha) \cdot \mathcal{C}_{topo}(\mathcal{E}_s, \mathcal{G})$$
(56)

where C_{sem} is semantic coherence, C_{topo} is topological coherence, and $\alpha \in [0,1]$ is a weighting parameter.

Theorem 4 (Generation Consistency with Concentration Bounds). The Enhancement Agent produces node v_s with attributes x_s and edges \mathcal{E}_s that satisfy:

1. Semantic consistency with concentration bounds:

$$\mathbb{P}\left(\left|\mathcal{C}_{sem}(x_s, \mathcal{X}) - \mathbb{E}[\mathcal{C}_{sem}(x_s, \mathcal{X})]\right| > t\right) \le 2\exp\left(-\frac{|\mathcal{K}_t|t^2}{2\sigma_{sem}^2}\right)$$
(57)

2. Topological consistency with respect to local and global network properties:

$$\mathbb{E}[\mathcal{C}_{topo}(\mathcal{E}_s, \mathcal{G})] \ge \beta \cdot \max_{v_j \in \mathcal{V}_k} \mathcal{C}_{topo}(\mathcal{E}_j, \mathcal{G}) - \frac{C_{\mathcal{G}}}{|\mathcal{K}_t|^{1/3}}$$
(58)

3. The generative mechanism preserves manifold structure in the asymptotic limit:

$$\lim_{|\mathcal{K}_t| \to \infty} \mathbb{P}\left(dist(x_s, \mathcal{M}_{\mathcal{X}}) > \epsilon\right) = 0$$
 (59)

where $\mathcal{M}_{\mathcal{X}}$ is the manifold on which the original node attributes lie.

Proof. Part 1: Semantic Consistency Concentration

The Enhancement Agent generates node attributes via a conditional autoregressive model:

$$P(x_s|\mathcal{K}_t, \mathcal{R}_t) = \prod_{i=1}^{L} P(x_s^i|x_s^{< i}, \mathcal{X}_k, \mathcal{E}_k, \mathcal{R}_t)$$
(60)

Each token generation can be decomposed as:

$$P(x_s^i | x_s^{< i}, \mathcal{X}_k, \mathcal{E}_k, \mathcal{R}_t) \propto \exp\left(\frac{\phi(x_s^i)^T \mathbf{h}_i}{\tau}\right)$$
 (61)

where \mathbf{h}_i is the contextualized representation and τ is a temperature parameter.

The contextualized representation integrates information from the knowledge encapsulation:

$$\mathbf{h}_i = \mathbf{W}_1 \cdot f(x_s^{< i}) + \mathbf{W}_2 \cdot g(\mathcal{X}_k) + \mathbf{W}_3 \cdot h(\mathcal{E}_k)$$
(62)

Let $C_{\text{sem}}(x_s, \mathcal{X}) = \max_{x_j \in \mathcal{X}} \mathcal{S}(x_s, x_j)$. The semantic similarity function \mathcal{S} satisfies the bounded differences condition:

$$|\mathcal{S}(x_s, x_i) - \mathcal{S}(x_s, x_{i'})| \le L_{\mathcal{S}} \cdot |x_i - x_{i'}| \tag{63}$$

By applying McDiarmid's inequality to the empirical semantic coherence, we establish the concentration bounds.

Part 2: Topological Consistency

The edge generation mechanism:

$$P((v_s, v_i) \in \mathcal{E}_c | \mathcal{K}_t, \mathcal{R}_t) = \sigma \left(\theta_1 \cdot \sin(x_s, x_i) + \theta_2 \cdot \frac{|\mathcal{N}(v_i) \cap \mathcal{N}_K(v_s)|}{|\mathcal{N}_K(v_s)|} + \theta_3 \cdot \frac{k_i}{\max_j k_j} \right)$$
(64)

We analyze the asymptotic properties using random graph theory. Let $G(n, p_{ij})$ be a random graph model where edge (i, j) exists with probability p_{ij} .

The expected clustering coefficient:

$$\mathbb{E}[CC(v_s)] = \frac{\sum_{i,j} p_{is} \cdot p_{js} \cdot p_{ij}}{\sum_{i,j} p_{is} \cdot p_{js}}$$

$$(65)$$

For our model:

$$p_{ij} = \sigma \left(\theta_1 \cdot \sin(x_i, x_j) + \theta_2 \cdot \frac{|\mathcal{N}(v_i) \cap \mathcal{N}(v_j)|}{|\mathcal{N}(v_i)|} + \theta_3 \cdot \frac{k_j}{\max_l k_l} \right)$$
(66)

The local-global consistency emerges from the balance between the three terms:

- θ_1 term preserves homophily (similar nodes connect)
- θ_2 term ensures triadic closure (friends of friends connect)
- θ_3 term maintains scale-free properties (preferential attachment)

Using graph limit theory, the topological consistency is governed by:

$$C_{\text{topo}}(\mathcal{E}_s, \mathcal{G}) \approx 1 - \frac{1}{2} |W_{\mathcal{E}_s} - W_{\mathcal{G}}| \square$$
 (67)

where $W_{\mathcal{E}s}$ and $W\mathcal{G}$ are graphons (limiting objects of graphs) and $|\cdot|_{\square}$ is the cut norm.

Part 3: Manifold Preservation

Let $\mathcal{M}_{\mathcal{X}} \subset \mathbb{R}^d$ be a compact r-dimensional manifold with condition number $1/\tau$ and reach at least $\tau > 0$. The nodes $\mathcal{X} = x_1, \dots, x_N$ are sampled from a distribution supported on $\mathcal{M}_{\mathcal{X}}$.

The language model learns a conditional distribution:

$$P_{\text{LLM}}(x|\mathcal{K}_t) = \frac{1}{Z(\mathcal{K}_t)} \exp\left(-\frac{\operatorname{dist}(x, \mathcal{M}_{\mathcal{X}}(\mathcal{K}_t))^2}{2\sigma^2}\right) \cdot P_{\text{prior}}(x)$$
 (68)

As $|\mathcal{K}t| \to \infty$, we have:

$$\mathcal{M}_{\mathcal{X}}(\mathcal{K}_t) \to \mathcal{M}_{\mathcal{X}}$$
 in the Hausdorff metric (69)

The manifold preservation follows from the consistency of kernel density estimators on manifolds and the properties of autoregressive language models.

Proposition 2 (Latent Variable Interpretation). The Enhancement Agent's generative process is equivalent to a controlled stochastic differential equation on the graph manifold:

$$dx_t = \mu(x_t, \mathcal{K}_t)dt + \sigma(x_t, \mathcal{K}_t)dW_t \tag{70}$$

where μ is a drift term aligning generation with the knowledge encapsulation, σ is a diffusion term controlling diversity, and W_t is a Wiener process.

Proof. We establish the equivalence by showing that the discrete token generation process converges to the SDE in the continuous limit. The proof uses techniques from the theory of diffusion models and score-matching generative models. \Box

I.3 Theoretical Properties of Quality Assessment and Convergence

We now establish rigorous guarantees for the Evaluation Agent's quality assessment and convergence determination capabilities.

Definition 4 (Marginal Quality Contribution). For a graph $\mathcal{G} = (\mathcal{V}, \mathcal{E}, \mathcal{X}, \mathcal{Y})$ and a generated node v_s with attributes x_s and connections \mathcal{E}_s , the marginal quality contribution is:

$$\Delta Q(v_s, \mathcal{G}) = Q(\mathcal{G} \cup \{v_s, \mathcal{E}_s\}) - Q(\mathcal{G}) \tag{71}$$

where Q is a quality functional measuring overall graph utility for the target task.

Theorem 5 (Quality Assessment with Statistical Guarantees). *The Evaluation Agent implements a quality assessment function that satisfies:*

1. Strong correlation with marginal quality contribution:

$$\mathbb{E}[\Delta Q(v_s, \mathcal{G})| LLM_V(v_s, \mathcal{R}_0, \mathcal{R}_t, \mathcal{K}_t) = q] = f(q) + O\left(\frac{1}{|\mathcal{V}|}\right)$$
(72)

where f is monotonically increasing and Lipschitz continuous.

2. Thresholding efficiency with probabilistic guarantees:

$$\mathbb{P}(\Delta Q(v_s, \mathcal{G}) > 0 | LLM_V(v_s, \mathcal{R}_0, \mathcal{R}_t, \mathcal{K}_t) > \tau_t) \ge 1 - \exp(-c \cdot |\mathcal{K}_t|) \tag{73}$$

for some constant c > 0 and appropriately chosen threshold τ_t .

3. Convergence detection with statistical significance:

$$\mathbb{P}(Converged_t = 1 | \mathbb{E}[\Delta Q_{t+1}] < \epsilon) \ge 1 - \delta \tag{74}$$

where δ decreases exponentially with the window size k in the convergence criterion.

Proof. Part 1: Correlation with Marginal Quality

The Evaluation Agent employs a multi-dimensional quality assessment:

$$LLM_V(v_s, \mathcal{R}_0, \mathcal{R}_t, \mathcal{K}_t) = g\left(\Phi_{sem}(v_s, \mathcal{K}_t), \Phi_{topo}(v_s, \mathcal{G}_t), \Phi_{bal}(v_s, \mathcal{Y}_t)\right)$$
(75)

The quality functional Q can be decomposed into semantic, topological, and balance components:

$$Q(\mathcal{G}) = \omega_1 Q_{\text{sem}}(\mathcal{G}) + \omega_2 Q_{\text{topo}}(\mathcal{G}) + \omega_3 Q_{\text{bal}}(\mathcal{G})$$
(76)

For each component, we establish bounds on the approximation error:

$$|\mathbb{E}\left[\Delta Q_{\text{sem}}(v_s, \mathcal{G}) \mid \Phi_{\text{sem}}(v_s, \mathcal{K}t) = s\right] - f_{\text{sem}}(s)| \le \frac{C_1}{|\mathcal{K}t|}$$
(77)

$$|\mathbb{E}\left[\Delta Q_{\text{topo}}(v_s, \mathcal{G}) \mid \Phi_{\text{topo}}(v_s, \mathcal{G}t) = t\right] - f_{\text{topo}}(t)| \le \frac{C_2}{|\mathcal{V}|}$$
(78)

$$|\mathbb{E}\left[\Delta Q_{\text{bal}}(v_s, \mathcal{G}) \mid \Phi_{\text{bal}}(v_s, \mathcal{Y}t) = b\right] - f_{\text{bal}}(b)| \le \frac{C_3}{\sqrt{|\mathcal{V}|}}$$
(79)

By the properties of the LLM's function approximation capabilities, we have:

$$|g - \omega_1 f_{\text{sem}} - \omega_2 f_{\text{topo}} - \omega_3 f_{\text{bal}}| \infty \le \epsilon_{\text{LLM}}$$
 (80)

Combining these bounds establishes the correlation with marginal quality.

Part 2: Thresholding Efficiency

The adaptive threshold mechanism:

$$\tau_t = \tau_{t-1} + \zeta(\bar{\mathcal{F}}_t(\omega_t^*) - \bar{\mathcal{F}}_{t-1}(\omega_{t-1}^*))$$
(81)

converges to an optimal threshold $\tau*$ that maximizes expected improvement:

$$\tau^* = \arg\max_{\tau} \mathbb{E}[\Delta Q(\mathcal{V}_{\text{accepted}}(\tau), \mathcal{G})]$$
 (82)

where $V_{\text{accepted}}(\tau) = v_s : \text{LLM}_V(v_s, \cdot) > \tau$.

By the properties of sub-Gaussian random variables and the Lipschitz continuity of f, we establish the high-probability guarantee on positive quality contribution.

Part 3: Convergence Detection

The convergence criterion:

$$Converged_{t} = \mathbb{I}\left(\max_{j \in 1, \dots, k} |\bar{\mathcal{F}}_{t}(\omega_{t}^{*}) - \bar{\mathcal{F}}_{t-j}(\omega_{t-j}^{*})| < \epsilon \wedge LLM_{goal}(\mathcal{R}_{0}, \mathcal{R}_{t}) = True\right)$$
(83)

implements a change-point detection algorithm with multiple hypothesis testing.

The probability of false convergence detection is bounded by:

$$\mathbb{P}(\mathsf{Converged}_t = 1 | \mathbb{E}[\Delta Q_{t+1}] \ge \epsilon) \le k \cdot \exp\left(-\frac{2n\epsilon^2}{C_Q^2}\right)$$
 (84)

where n is the number of samples used to estimate $\bar{\mathcal{F}}_t$ and C_Q is a bound on the quality range.

Likewise, the probability of missing convergence is bounded by:

$$\mathbb{P}(\mathsf{Converged}_t = 0 | \mathbb{E}[\Delta Q_{t+1}] < \epsilon/2) \le \exp\left(-\frac{n\epsilon^2}{8C_Q^2}\right)$$
 (85)

The combined error probability decays exponentially with the sample size and window length. \Box

Corollary 2 (Optimal Stopping Property). *The Evaluation Agent's convergence criterion implements an approximately optimal stopping rule for the synthesis process, achieving a regret bound of:*

$$Regret(T) \le O\left(\sqrt{T\log T}\right)$$
 (86)

where T is the maximum number of iterations.

Proof. We frame the convergence determination as a multi-armed bandit problem with non-stationary rewards, where the arms correspond to continue/stop decisions. Applying results from optimal stopping theory and the regret analysis of UCB algorithms yields the result.

I.4 Unified Multi-Agent System Dynamics

We now establish theoretical results concerning the collective behavior of the agent system, framing it as optimization on a Riemannian manifold.

Definition 5 (Graph Configuration Manifold). *The space of possible graph configurations forms a Riemannian manifold \mathcal{MG} with metric tensor:*

$$g_{ij}(\mathcal{G}) = \mathbb{E}\left[\frac{\partial \log p(\mathcal{G}|\theta)}{\partial \theta_i} \frac{\partial \log p(\mathcal{G}|\theta)}{\partial \theta_j}\right]$$
(87)

where $p(G|\theta)$ is a parametric model of graph distribution and θ are the parameters.

Theorem 6 (Manifold Optimization Dynamics). The multi-agent system in GraphMaster implements natural gradient ascent on the graph configuration manifold $\mathcal{M}_{\mathcal{G}}$, optimizing a multi-objective function:

$$\Psi^*(\mathcal{G}) = \lambda_1 \Psi sem(\mathcal{G}) + \lambda_2 \Psi_{ctruct}(\mathcal{G}) + \lambda_3 \Psi_{bal}(\mathcal{G})$$
(88)

with adaptive weights λ_i that evolve according to:

$$\lambda_i^{t+1} = \Pi_{\Delta} \left[\lambda_i^t + \eta \nabla_{\lambda_i} P(\mathcal{G}_t) \right]$$
 (89)

where $\Pi\Delta$ is projection onto the probability simplex.

The convergence rate is:

$$\mathbb{E}[\Psi^*(\mathcal{G}^*) - \Psi^*(\mathcal{G}_T)] \le O\left(\frac{1}{\sqrt{T}}\right) \tag{90}$$

for a non-convex objective, and:

$$\mathbb{E}[\Psi^*(\mathcal{G}^*) - \Psi^*(\mathcal{G}_T)] \le O\left(\frac{\log T}{T}\right) \tag{91}$$

if the objective satisfies Polyak-Łojasiewicz conditions.

Proof. Part 1: Natural Gradient Dynamics

At each iteration, the system performs:

$$\mathcal{G}t + 1 = \Pi \mathcal{M}_{\mathcal{G}} \left[\mathcal{G}_t + \eta_t \cdot \mathcal{I}^{-1}(\mathcal{G}_t) \cdot \nabla \Psi^*(\mathcal{G}_t) \right]$$
(92)

where $\mathcal{I}(\mathcal{G}_t)$ is the Fisher information matrix and $\Pi \mathcal{M}_{\mathcal{G}}$ is projection onto the manifold.

This update is implemented by the collaborative agent process:

$$\mathcal{K}_t = \Phi(\mathcal{G}_t) \tag{93}$$

$$\mathcal{V}_s^t = \text{LLM}_E(\mathcal{K}_t, \mathcal{R}_t, M_t) \tag{94}$$

$$\mathcal{E}_s^t = \left\{ (v_s, v_i) \mid P((v_s, v_i) \mid \mathcal{K}_t, \mathcal{R}_t) > \eta_t \right\} \tag{95}$$

$$\mathcal{V}_{\text{accepted}}^{t} = \left\{ v_s \in \mathcal{V}_s^{t} \mid \text{LLM}_V(v_s, \mathcal{R}_0, \mathcal{R}_t, \mathcal{K}_t) > \tau_t \right\}$$
(96)

$$\mathcal{G}_{t+1} = \mathcal{G}_t \oplus \left(\mathcal{V}_{\text{accepted}}^t, \mathcal{E}_s^t \big|_{\mathcal{V}_{\text{accepted}}^t} \right)$$
(97)

Part 2: Adaptive Weight Dynamics

The Manager Agent implements online gradient-based multi-objective optimization:

$$\lambda_i^{t+1} = \Pi_{\Delta} \left[\lambda_i^t + \eta \nabla_{\lambda_i} P(\mathcal{G}_t) \right]$$
(98)

where $P(\mathcal{G}_t)$ measures progress toward synthesis objectives.

This follows the Multiple Gradient Descent Algorithm (MGDA) for Pareto optimization:

$$\nabla_{\lambda_i} P(\mathcal{G}t) \approx \nabla_{\lambda_i} \min_{j} \frac{\Psi_j(\mathcal{G}_t) - \Psi_j(\mathcal{G}_0)}{\Psi_j^* - \Psi_j(\mathcal{G}_0)}$$
(99)

Part 3: Convergence Analysis

For a general non-convex objective, we have:

$$\mathbb{E}\left[\min_{t=0,1,...,T-1} |\nabla \Psi^*(\mathcal{G}_t)|^2\right] \le \frac{2[\Psi^*(\mathcal{G}^*) - \Psi^*(\mathcal{G}_0)]}{\eta T} + \frac{\eta L}{2}$$
(100)

For appropriately chosen step size $\eta = O(1/\sqrt{T})$, this yields the $O(1/\sqrt{T})$ convergence rate.

If the objective satisfies the Polyak-Łojasiewicz condition:

$$|\nabla \Psi^*(\mathcal{G})|^2 \ge 2\mu [\Psi^*(\mathcal{G}^*) - \Psi^*(\mathcal{G})] \tag{101}$$

for some $\mu>0,$ then we obtain the improved $O(\frac{\log T}{T})$ rate.

Theorem 7 (Spectral Convergence of Synthesized Graphs). Let \mathcal{G}_{orig} be the original graph and \mathcal{G}_{synth} be the synthesized graph after convergence. Under appropriate conditions on the synthesis process, the eigenvalue distributions of their normalized Laplacians converge:

$$\lim_{|\mathcal{V}| \to \infty} d_{LP}(\rho_{\mathcal{G}_{orig}}, \rho_{\mathcal{G}_{synth}}) = 0 \tag{102}$$

where d_{LP} is the Lévy-Prokhorov metric between spectral distributions and $\rho_{\mathcal{G}}$ is the empirical spectral distribution of graph \mathcal{G} .

Proof. We establish this result by analyzing the perturbation of the graph spectrum under node additions. The proof relies on matrix concentration inequalities and recent results in random matrix theory concerning deformed Wigner matrices.

For graphs with bounded degree, the spectral distribution satisfies a semicircle law in the limit. The synthesis process preserves this property through controlled edge formation that maintains degree distribution and local clustering patterns.

These theoretical results collectively establish the mathematical foundations underlying GraphMaster's effectiveness, providing formal guarantees for its information preservation, generation quality, evaluation accuracy, and convergence properties. The integration of concepts from information theory, statistical learning, manifold optimization, and spectral graph theory creates a comprehensive theoretical framework that explains why our multi-agent approach succeeds in generating high-quality text-attributed graphs in data-limited environments.

J Limitations and Future Work

While GraphMaster demonstrates significant advances in text-attributed graph synthesis, several important limitations remain. The current background knowledge selection mechanism, while effective for moderate-sized graphs, faces challenges with very large or heterogeneous graph structures. Specifically, our Personalized PageRank-based approach may prioritize structurally central nodes while potentially undersampling semantically important but topologically peripheral communities. This sampling bias can result in synthesis blind spots, particularly in graphs with highly skewed degree distributions or multiple disconnected components with distinct semantic characteristics. Additionally, the quality evaluation process relies on LLM capabilities that exhibit variance across different base models and parameter scales. This interdependence creates challenges for deployment in resource-constrained environments where smaller models are preferable. Computational requirements present another significant limitation. The multi-agent architecture, while theoretically elegant, incurs substantial inference overhead as each agent performs multiple LLM calls per synthesis round. For extremely large graphs, the current approach requires non-trivial batching strategies and optimization techniques that may not be readily available in standard deployment scenarios.

For future work, we envision several promising research directions. First, hierarchical multiresolution synthesis could revolutionize the approach by simultaneously modeling graph characteristics at multiple levels of abstraction–from global topological patterns to local semantic neighborhoods. This layered perspective would enable more coherent synthesis that preserves both macro-structure and micro-semantics while potentially reducing computational complexity through selective refinement. Second, cross-domain knowledge transfer represents a frontier challenge, where synthesis agents could leverage patterns learned from data-rich domains to enhance generation in data-scarce domains without explicit domain adaptation. This would require fundamental advances in domainagnostic graph representations that capture universal structural and semantic patterns transferable across vastly different graph types. Rather than relying on fixed sampling algorithms, the framework could develop adaptive sampling policies optimized specifically for the synthesis objective. Finally, exploring emergent graph properties from synthesis could yield insights into how locally generated elements collectively produce global graph characteristics that were never explicitly modeled-potentially revealing new theoretical connections between local generation rules and emergent network phenomena. These developments would not only address current limitations but could fundamentally reshape our understanding of generative modeling for complex relational data structures.

K Case Study

In this study, we conducted a case study to track the entire synthesis framework and documented the complete enhancement process. Table 7 presents the background knowledge possessed by our Perception Agent prior to generating the environmental perception report, which serves as a critical basis for the environmental status report generated in Table 8. In Table 8, not only is the environmental status report produced, but the Manager Agent's decision for the current round—namely, semantic enhancement—is also provided. Subsequently, based on the information from the semantic enhancement, the Perception Agent conducted a sampling of the background knowledge nodes, as illustrated in Table 9 (for brevity, only two nodes are displayed). Following this, Table 10 presents the node information generated by our Enhancement Agent (owing to space limitations, the abstracts of some nodes have been omitted). Finally, Table 11 exhibits the quality evaluation of the generated nodes by our Evaluation Agent. As indicated in the table, the newly generated "new_node 5" was omitted due to substandard quality, and the table further demonstrates that the Evaluation Agent judges the entire synthesis process as not yet converged, necessitating continuation to the next round of enhancement.

Table 7: Semantic Enhancement Case Study

```
Dataset: <SubCora>
Initial text attribute graph features:
"Graph": { "num_nodes": 1354,
"num_edges": 2486,
"avg_degree": 3.672082717872969,
"density": 0.002714030094510694,
"clustering coefficient": 0.2296011350131079,
"avg path length": 6.52047030925269,
"connected components": 78,
"largest component size": 1223,
"indices": [4, 2, 1, 3, 18, 11, 6, 15, 12, 9, 16, 10, 5, 13, 7, 17, 8, 20, 21, 24, 22, 23, 19, 36, 29,
27, 33, 47, 79, 25, 26, 30, 31, 34, 35, 37, 38, 40, 45, 50, 52, 53, 55, 56, 59, 62, 64, 66, 67, 73,
77, 80, 83, 28, 32, 39, 41, 42, 43, 44, 46, 48, 49, 51, 54, 57, 58, 60, 61, 63, 65, 68, 69, 70, 71,
72, 74, 75, 76, 78, 81, 82, 84, 85, 86, 87, 88, 89, 90, 91, 92, 93, 94, 95, 96, 97, 98, 0, 14],
"sizes": [192, 106, 97, 84, 78, 76, 74, 71, 65, 56, 55, 46, 42, 37, 35, 33, 18, 15, 14, 14, 10, 10,
1, 1, 1],
"distribution": {"4": 192, "2": 106, "1": 97, "3": 84, "18": 78, "11": 76, "6": 74, "15": 71,
"12": 65, "9": 56, "16": 55, "10": 46, "5": 42, "13": 37, "7": 35, "17": 33, "8": 18, "20": 15,
"21": 14, "24": 14, "22": 10, "23": 10, "19": 9, "36": 6, "29": 5, "27": 3, "33": 3, "47": 3,
"79": 3, "25": 2, "26": 2, "30": 2, "31": 2, "34": 2, "35": 2, "37": 2, "38": 2, "40": 2, "45": 2,
"50": 2, "52": 2, "53": 2, "55": 2, "56": 2, "59": 2, "62": 2, "64": 2, "66": 2, "67": 2, "73": 2,
"77": 2, "80": 2, "83": 2, "28": 1, "32": 1, "39": 1, "41": 1, "42": 1, "43": 1, "44": 1, "46": 1,
"48": 1, "49": 1, "51": 1, "54": 1, "57": 1, "58": 1, "60": 1, "61": 1, "63": 1, "65": 1, "68": 1,
"69": 1, "70": 1, "71": 1, "72": 1, "74": 1, "75": 1, "76": 1, "78": 1, "81": 1, "82": 1, "84": 1,
"85": 1, "86": 1, "87": 1, "88": 1, "89": 1, "90": 1, "91": 1, "92": 1, "93": 1, "94": 1, "95": 1,
"96": 1, "97": 1, "98": 1, "0": 1, "14": 1},
"statistics": {
"4": {
"size": 192,
"internal edges": 423,
"fraction_of_graph": 0.14180206794682423,
"modularity contribution": 0.103009273492297
},
"2": {
"size": 106,
"internal edges": 156,
"fraction of graph": 0.07828655834564253,
"modularity contribution": 0.05272713033696666
},
\ "StructuralDistribution": \ "degree distribution": \ \ "4": 233, "14": 4,"7": 33,"3": 273,"5":
127,"31": 1, ...,
"SemanticDistribution": { "placeholder": "Semantic distribution analysis would go here" }, "LabelDistribution": { "2": 410, "4": 110, "6": 175, "1": 208, "3": 214, "5": 90, "0": 147 }, "ClassStatistics": { "2": { "count": 410, "fraction": 0.30280649926144754, "internal_edges":
518, "avg_degree": 2.526829268292683, "community_distribution": { "18": 26, "2": 20,} }
..., } }
```

Table 8: Semantic Enhancement Case Study

Dataset: <SubCora>

Initial Environment Report:

Summary:{

The graph under analysis contains 1,354 nodes and 2,486 edges, resulting in a sparse but structured topology with an average degree of 3.67 and an overall graph density of 0.0027. Such characteristics are typical in real-world networks, where the number of edges scales sub-quadratically with the number of nodes. The average shortest path length of 6.52 indicates that the network is relatively well-connected in its largest component, despite the overall sparsity. The clustering coefficient, a measure of local cohesiveness, is 0.23, suggesting that nodes tend to form tight-knit neighborhoods—an important property for tasks that rely on local structural features, such as label propagation and GNN-based message passing. Structurally, the graph is partitioned into 78 connected components, but it is worth noting that the largest connected component comprises 1,223 nodes, accounting for over 90% of the entire graph. This makes the graph effectively connected for most practical purposes, enabling global information diffusion across the majority of nodes. Community detection reveals a complex and heterogeneous modular organization. There are several large communities, such as those of size 200, 112, 97, and 96, indicating strong intra-community connectivity in core regions. These large communities contribute significantly to the overall modularity, with notable examples such as community "4" (size 200, modularity contribution ≈ 0.1052) and "3" (size 112, contribution ≈ 0.0631). However, the long tail in the community size distribution is striking:

1)Over 40 communities consist of only 1 or 2 nodes,

2)More than 60% of communities are smaller than size 10.

This imbalance in community sizes suggests that while the graph's topology supports clear structural groupings in dense areas, it also contains many fragmented or peripheral regions that are less well-served by structural clustering alone. These small communities may represent semantic outliers, conceptually related nodes that are not densely connected in the topology. Overall, the graph structure is well-organized, with a solid backbone of connectivity and modular clusters. The community detection result aligns with expectations in real-world data but also reveals opportunities for further refinement—particularly in regions where structure alone fails to form meaningful communities.

Given this context, incorporating semantic node features (e.g., textual content, embeddings, or metadata) could greatly complement the topological view. Nodes in small or singleton communities may be structurally isolated but semantically similar, and semantic enhancement can help bridge this gap, improving community coherence, label consistency, and downstream task performance such as classification, recommendation, and contrastive learning.

Manager Agent's Decision: {Semantic Enhancement}

```
Dataset: <SubCora>
Perception Agent Knowledge Extraction:
Graph<sub>Sub</sub>: {
"node_id": 536,
"label": 0,
"text": "Title: Dynamic Constraint Satisfaction using Case-Based Reasoning Techniques \n
Abstract: The Dynamic Constraint Satisfaction Problem (DCSP) formalism has been gaining
attention as a valuable and often necessary extension of the static CSP framework. Dynamic
Constraint Satisfaction enables CSP techniques to be applied more extensively, since it can
be applied in domains where the set of constraints and variables involved in the problem
evolves with time. At the same time, the Case-Based Reasoning (CBR) community has been
working on techniques by which to reuse existing solutions when solving new problems.
We have observed that dynamic constraint satisfaction matches very closely the case-based
reasoning process of case adaptation. These observations emerged from our previous work on
combining CBR and CSP to achieve a constraint-based adaptation. This paper summarizes
our previous results, describes the similarity of the challenges facing both DCSP and case
adaptation, and shows how CSP and CBR can together begin to address these chal lenges.",
"neighbors": [
639
"mask": "Train"
"node_id": 41,
"label": 0.
"text": "Title: A Memory Model for Case Retrieval by Activation Passing \n Abstract: We
present a tree-structured architecture for supervised learning. The statistical model underlying
the architecture is a hierarchical mixture model in which both the mixture coefficients and
the mixture components are generalized linear models (GLIM's). Learning is treated as a
maximum likelihood problem; in particular, we present an Expectation-Maximization (EM)
algorithm for adjusting the parameters of the architecture. We also develop an on-line learning
algorithm in which the parameters are updated incrementally. Comparative simulation results
are presented in the robot dynamics domain. This report describes research done at the Dept.
of Brain and Cognitive Sciences, the Center for Biological and Computational Learning, and
the Artificial Intelligence Laboratory of the Massachusetts Institute of Technology. Support
for CBCL is provided in part by a grant from the NSF (ASC-9217041). Support for the
laboratory's artificial intelligence research is provided in part by the Advanced Research
Projects Agency of the Dept. of Defense. The authors were supported by a grant from the
McDonnell-Pew Foundation, by a grant from ATR Human Information Processing Research
Laboratories, by a grant from Siemens Corporation, by by grant IRI-9013991 from the
National Science Foundation, by grant N00014-90-J-1942 from the Office of Naval Research,
and by NSF grant ECS-9216531 to support an Initiative in Intelligent Control at MIT. Michael
I. Jordan is a NSF Presidential Young Investigator. ",
"neighbors": [
166,
637,
761,
1004,
1005,
1116,
1196
"mask": "Train"
},
```

}

```
Dataset: <SubCora>
Enhancement Agent generates high-quality nodes:
"node_id": "new_node 1",
"label": 0,
"text": "Title: Integrating Explanation-Based Learning with Case Adaptation Strategies\n
Abstract: This paper presents a novel approach to case adaptation in case-based reasoning
systems by integrating explanation-based learning techniques. Traditional case adaptation
relies heavily on domain-specific adaptation rules that are often difficult to acquire and main-
tain. Our approach uses explanations generated during problem-solving to identify adaptation
patterns and generalize them into reusable adaptation strategies. We demonstrate how these
strategies can be applied across different domains with minimal knowledge engineering effort.
Experimental results show that the integrated approach improves adaptation performance
in comparison to rule-based adaptation methods, especially in domains where adaptation
knowledge is incomplete or rapidly evolving. The paper presents a formal framework for the
approach and discusses its implementation in a case-based planning system.",
"neighbors": [337, 833, 639, 476],
"mask": "Train"
"node id": "new node 2",
"label": 1.
"text": "Title: Adaptive Parameter Control in Evolution Strategies for Dynamic
Environments\n Abstract: Omitted due to table size limitation.",
"neighbors": [462, 70, 1312],
"mask": "Train"
"node id": "new node 3",
"label": 0,
"text": "Title: Multi-Level Similarity Assessment for Case Retrieval in Heterogeneous
Domains\n Abstract: Omitted due to table size limitation.",
"neighbors": [637, 638, 825, 1004],
"mask": "Train"
"node id": "new node 4",
"label": 3,
"text": "Title: Hybrid Neural-Symbolic Architecture for Interpretable Knowledge
Extraction\n Abstract: Omitted due to table size limitation.",
"neighbors": [1290, 263],
"mask": "Train"
},
"node_id": "new_node 5",
"label": 0.
"text": "Title: Case-base Design for Knowledge Discovery\n Abstract: Case Based Rea-
soning has proven to be useful for AI systems. Our research introduces a new method
called KDD-CBR (Knowledge Discovery through Database Case-Based Reasoning) which
combines data mining with case bases for information retrieval and management. The system
works by analyzing patterns in large datasets and then applies unique non-traditional methods
for case storage. Unlike other approaches, we focus on pattern recognition instead of adapta-
tion or similarity, which makes our approach completely novel in the field. Tests show this
approach has better inference capability than other CBR techniques in some instances but
worse in others. The implications for future research directions are significant and should
be explored further with additional funding and more test cases. Additionally, we plan to
integrate KDD-CBR with deep neural networks to further enhance performance on arbitrary
datasets.",
"neighbors": [462, 70, 1017],
                                           46
"mask": "Train"
```

```
Dataset: <SubCora>
Evaluation Agent evaluates node quality and determines whether it has converged.:
"node_id": "new_node 1",
"label": 0,
"text": "Title: Integrating Explanation-Based Learning with Case Adaptation Strategies\n
Abstract: This paper presents a novel approach to case adaptation in case-based reasoning
systems by integrating explanation-based learning techniques. Traditional case adaptation
relies heavily on domain-specific adaptation rules that are often difficult to acquire and
maintain. Our approach uses explanations generated during problem-solving to identify
adaptation patterns and generalize them into reusable adaptation strategies. We demonstrate
how these strategies can be applied across different domains with minimal knowledge
engineering effort. Experimental results show that the integrated approach improves
adaptation performance in comparison to rule-based adaptation methods, especially in
domains where adaptation knowledge is incomplete or rapidly evolving. The paper presents a
formal framework for the approach and discusses its implementation in a case-based planning
system.",
"neighbors": [337, 833, 639, 476],
"mask": "Train"
"node_id": "new_node 2",
"label": 1.
"text": "Title: Adaptive Parameter Control in Evolution Strategies for Dynamic Environments
\n Abstract: Omitted due to table size limitation.",
"neighbors": [462, 70, 1312],
"mask": "Train"
"node id": "new node 3",
"label": 0,
"text": "Title: Multi-Level Similarity Assessment for Case Retrieval in Heterogeneous
Domains \n Abstract: Omitted due to table size limitation.",
"neighbors": [637, 638, 825, 1004],
"mask": "Train"
},
"node id": "new node 4",
"label": 3,
"text": "Title: Hybrid Neural-Symbolic Architecture for Interpretable Knowledge Extraction
\n Abstract: Omitted due to table size limitation.",
"neighbors": [1290, 263],
"mask": "Train"
Summary: { After checking the node quality based on the background knowledge and
environment report, delete new_node 5.
According to the status check, the entire synthesis process has not converged and needs to
continue to the next round of enhancement. }
```